DEVELOPMENT AND VALIDATION OF A PREDICTIVE MODEL TO ASSESS THE IMPACT OF COASTAL OPERATIONS ON URBAN SCALE AIR QUALITY

SERDP Project Number
SI-1253

Performing Organization
Desert Research Institute
2215 Raggio Parkway
Reno, NV 89512

Lead Principal Investigator
Dr. Alan W. Gertler

Date
September 29, 2006

Approved for public release; distribution is unlimited

REPORT DOCUMENTATION PAGE

Form Approved
OMB No. 0704-0188

PLEASE DO NOT RETURN YOUR FORM TO THE ABOVE ORGANIZATION.

1. REPORT DATE *(DD-MM-YYYY)*	2. REPORT TYPE	3. DATES COVERED *(From - To)*
29-09-2006	Final	06/26/02 to 12/31/05

4. TITLE AND SUBTITLE

Development and Validation of a Predictive Model to Assess the Impact of Coastal Operations On Urban Scale Air Quality

5a. CONTRACT NUMBER

DACA72-02-C-0008

5b. GRANT NUMBER

5c. PROGRAM ELEMENT NUMBER

6. AUTHOR(S)

Gertler, Alan W., Kahyaoğlu-Koračin, Julide, Koračin, Darko, Luria, Menachem, Stockwell, William, Weinroth, Erez

5d. PROJECT NUMBER

SI-1253

5e. TASK NUMBER

5f. WORK UNIT NUMBER

7. PERFORMING ORGANIZATION NAME(S) AND ADDRESS(ES)

Desert Research Institute
2215 Raggio Parkway
Reno, NV 89721

8. PERFORMING ORGANIZATION REPORT NUMBER

9. SPONSORING/MONITORING AGENCY NAME(S) AND ADDRESS(ES)

USAC, Humphreys Engr CTR SPT Activity
Attn: CEHEC - CT
7701 Telegraph Road
Alexandria, VA 22315-3660

10. SPONSOR/MONITOR'S ACRONYM(S)

DOD - SERDP

11. SPONSOR/MONITOR'S REPORT NUMBER(S)

12. DISTRIBUTION/AVAILABILITY STATEMENT

Distribution Statement A: Approved for Public Release, Distribution is Unlimited. Prepared in cooperation with the Tennessee Valley Authority

13. SUPPLEMENTARY NOTES

14. ABSTRACT

Many areas suffering from elevated pollutant levels are located in regions where there is significant uncertainty in predicting pollutant transport and dispersion (e.g., coastal zones). Traditional approaches to assess the impact of emissions in complex environments have included the application of statistical, Gaussian dispersion, single chemical box, Lagrangian, and Eulerian models. Each of these models has distinct advantages and disadvantages. This report describes the development of a meteorological air quality model with in-line chemistry that combines the advantages of the Eulerian and Lagrangian models. As part of the model validation, simulation results for a case study in the San Diego area of southwestern California are also discussed.

15. SUBJECT TERMS

Air quality modeling, coastal meteorology, atmospheric chemistry, emissions modeling, model validation

16. SECURITY CLASSIFICATION OF:			17. LIMITATION OF ABSTRACT	18. NUMBER OF PAGES	19a. NAME OF RESPONSIBLE PERSON
a. REPORT	b. ABSTRACT	c. THIS PAGE			Dr. Alan Gertler
U	U	U	UU	48	19b. TELEPHONE NUMBER *(Include area code)* 775-674-7061

Reset

Standard Form 298 (Rev. 8/98)
Prescribed by ANSI Std. Z39.18

Table of Contents

List of Figures

List of Tables

List of Acronyms

ASL	Above Sea Level
BL	Boundary layer
CALMET	a diagnostic 3-dimensional meteorological model and the meteorological preprocessor for CALPUFF
CALPUFF	a Lagrangian puff dispersion model
CAM-x	Comprehensive Airshed Model with Extensions
CARB	California Air Resources Board
CO	Carbon monoxide
COAMPS	Coupled Ocean Atmosphere Modeling Prediction system
DoD	Department of Defense
DRI	Desert Research Institute
EPA	Environmental Protection Agency
FT	Free troposphere
GVRD	Greater Vancouver Regional District
HNO_3	Nitric acid
ISCST	Industrial Source Complex – Short Term
LAP	Lagrangian particle
LAP model	Lagrangian particle model
LST	Local Standard Time
MM5	Meteorological Mesoscale Model 5
NCAR	National Center for Atmospheric Research
NO	Nitrogen oxide
NO_2	Nitrogen dioxide
NO_x	Oxides of nitrogen ($NO + NO_2$)
NO_y	Total nitrogen species (includes nitric acid, peroxyacetyl nitrate, nitrate, NO, and NO_2)
NO_z	NO_Y-NO_X
NOAA	National Oceanographic and Atmospheric Administration
NPS	Naval Postgraduate School
O_3	Ozone
OZIP	Ozone Isopleth Plotting program
PAN	Peroxyacetyl nitrate
PM	Particulate matter
PM_{10}	Particulate matter of aerodynamic diameter of 10 μm or less
$PM_{2.5}$	Particulate matter of aerodynamic diameter of 2.5 μm or less
ppbv	Part per billion -volume
ppm	Part per millsion
PSU	the Pennsylvania State University
RACM	Regional atmospheric chemistry mechanism
RADM	Regional acid deposition model
SBOX	a box chemistry simulation model
SCOS `	Southern California Oxidants study

SDAPCD	San Diego Air Pollution Control District
SERDP	Strategic Environmental Research and Defense Program
SON	Statement of Need
SO_2	Sulfur dioxide
TEII	Thermo Environmental Instruments Inc.
TEOO	Thermo Environmental Instruments, Inc.
TOG	Total organic gases (hydrocarbons)
TVA	Tennessee Valley Authority
UAM	Urban Airshed Model
UV	ultra violet
VOC	Volatile organic carbon (i.e., hydrocarbons)
WDD	Wind Direction
WDS	Wind Speed

Acknowledgements

Many individuals contributed to the success of this study. We would like to acknowledge the numerous DRI contributors including Dr. Darko Koračin and his research group (Travis McCord, Domagoj Podnar, and Ramesh Vellore) for their assistance with the Lagrangian particle model, Dr. Julide Kahyaoğlu-Koračin for performing the MM5 runs and preparing the emissions inventory, Dr. John Sagebiel for assistance with the emissions inventory, Dr. John Lewis for providing the meteorological forecasts, and Dr. William Stockwell and Irene Shumyatsky for their assistance with the Eulerian chemical model and CAMx runs. Dr. Menachem Luria led the aircraft component of the study with assistance from TVA (Dr. Roger Tanner, Ray Valente, S.T. Bairai, Vince Van Pelt, and David Branscomb) and for providing many key suggestions throughout the project. Dr. Erez Weinroth of DRI deserves a special acknowledgement for his work on developing the model linkage and performing the hybrid model analyses. From the California Air Resources Board, Dr. Vlad Isacov provided the Barrio Logan Tracer Experiment data and Dr. Paul Allen aided with the preparation of the emissions inventory. Dr. Paul Miller of the Naval Postgraduate School collaborated on the real-time MM5 forecasts. Assistance with HYSPLIT-chem was provided by Drs. Ariel Stein and Roland Draxler of NOAA. Finally, we would like to acknowledge the support of SERDP, under contract SI-1253 and Dr. Robert Holst, the program manager.

Executive Summary

Background and Objectives

Elevated levels of ozone (O_3) remain a serious issue throughout the U.S. Approximately 90 urban areas in the U.S., containing some 30% of the U.S. population, still exceed the O_3 standard, with little immediate prospect of attainment. All the major urban areas in California are classified as non-attainment for O_3. Control of O_3 in the troposphere is complicated by the fact that it is a secondary pollutant. Particulate matter (PM) is also a serious environmental issue. Recognizing the health impacts of fine particulates, i.e., $PM_{2.5}$, there are new standards for $PM_{2.5}$. Unlike PM_{10}, a significant fraction of ambient $PM_{2.5}$ is produced by secondary reactions.

Many of the urban areas classified as non-attainment for O_3 or PM_{10} and facing non-attainment for $PM_{2.5}$ are located along the east and west coasts of the U.S. and are home to major DoD facilities. These operations can be significant sources of the O_3 and $PM_{2.5}$ forming precursors, direct $PM_{2.5}$ and PM_{10} emissions, and emissions of toxic species. Much of the uncertainty in developing an understanding of the causes of reduced air quality in urban areas is due to uncertainty in the emissions inventories; however, in coastal areas the situation is confounded by the complex meteorology associated with the land/sea interface.

To evaluate the impact of emissions from DoD activities and control elevated pollutant levels, there is a need to develop forecasting models that incorporate the processes leading to secondary pollutant formation. These processes include emissions, meteorology (transport and dispersion), and transformation chemistry. In order to address this need, the primary objective of this study was to develop a prognostic modeling system capable of assessing the potential influence of DoD facilities and operations on air quality in coastal zones. An additional objective was to develop an approach applicable to other complex environments.

Methods

Currently there are three approaches to model transport, dispersion, and transformation of pollutants. These include Eulerian, Lagrangian, and hybrid approaches. Briefly, the Eulerian method divides the atmosphere into fixed grid cells for which the continuity equation is solved. This approach is used to represent the primary processes affecting chemical transformations; however, while the chemistry is well represented, dispersion and transport is limited by the size of the grid cells employed. This can lead to appreciable numerical errors.

The Lagrangian approach is generally used for non-reactive species and avoids the computational complexities associated with the simulation of the chemical reactions. This leads to improved performance in assessing transport and dispersion. Lagrangian models describe a hypothetical air parcel that is carried along the air parcel trajectory. Only first-order chemical reactions can be incorporated under this approach.

The hybrid approach combines the strengths of both the Eulerian and Lagrangian methods and may provide a unique approach for the next generation of chemical transport simulations. Current hybrid models use a simplified chemistry and the chemistry and transport/dispersion are lumped together, making it difficult to modify the modules.

The components of the hybrid model we developed include the following: Mesoscale Meteorological Module 5 (MM5) for the meteorological fields, a Lagrangian particle (LAP) model for advection and dispersion, and an Eulerian chemical model within the Linkage module for the transformations. The Linkage module couples the Lagrangian and Eulerian parts of the model. Another key component is the emissions inventory for the region. Brief descriptions of the components follow:

- **Mesoscale Meteorological Module:** MM5, the Fifth-Generation Pennsylvania State University (PSU)/National Center for Atmospheric Research (NCAR) prognostic meso-meteorological model. MM5 is non-hydrostatic, fully compressible, and uses terrain-influenced, vertical sigma-coordinates on a nested horizontal, rectangular staggered-grid.
- **Transport and Dispersion Module:** Meteorological input to the LAP includes 3-D wind fields, as well as the potential temperature. Advection and dispersion calculations are made in a Lagrangian framework. Meteorological input data were based on MM5 and the LAP uses the same map projection as MM5. Emission sources of various geometries including elevated and moving sources with arbitrary time-variable or time limited emission rates can be modeled.
- **Chemistry Module:** Based on the Regional Atmospheric Chemistry Mechanism (RACM). There are a total of 237 reactions in the RACM mechanism. Simulations were performed using a box model.
- **Lagrangian-Eulerian Linkage:** The linkage between the Eulerian and Lagrangian components is based on the concept of a concentration grid cell. An enhancement was needed for the LAP model to produce a particle specific "name" (ID) for each particle. This enables us to link each particle to a specific set of attributes (i.e., location, meteorological fields, and chemical composition). We assumed the LAP particles had different compositions based on their original source. A unique feature of this approach has enabled us to trace any particle at any given time back to its origin and to observe its transformation over time and space.

  The way the linkage works is for each time step and grid cell the particles are disaggregated and the different chemical species are then distributed within the grid cell. At this point the chemical model is applied. At the end of each time step (1-hr, the same time step as the output from the LAP model), new concentrations within each grid cell are predicted. Apportionment of the chemical concentrations to the individual original particles is made by weighted average. Distribution of newly produced chemical species is based on the diffusion time scale, mixing height, and turbulence intensity.
- **Emission inventory:** The inventory was based on the Southern California Oxidant study (SCOS) 1997 day-specific emissions inventory and the California Air Resources Board (CARB) annual inventory. Species included NO_x, SO_x, CO, PM, and total organic gases (TOG) for all sources, including on-road and off-road mobile sources, industrial sources, commercial and U.S. Navy marine vessels, and commercial, civil, and military aircrafts. The biogenic component of the inventory was recalculated for the validation period using observed temperatures and day-specific solar radiation values.

In order to obtain data for model validation, a total of 10 research flights were carried out during the period of July 7 to 25, 2003. The flights began at shortly before noon and lasted

approximately 5 hours. The flights covered an area of approximately 100 x 100 km with the San Diego harbor being the southwest corner of the domain. Measurements included NO, NO_2, NO_x, NO_y, SO_2, CO, O_3, light scattering, speciated hydrocarbons and aldehydes, pressure, temperature, humidity, and wind speed and direction.

Results and Accomplishments

Model Validation

One of the advances of this study was the methodology developed to validate the model predictions using the aircraft data. Traditionally, model output is presented for a specified time period (e.g., for the whole domain at a specific hour); however, the aircraft data is taken over a number of hours across a large spatial domain. In order to compare these predicted vs. observed results, we first modeled the pollutant concentrations for each particle during each hour of the flight period. A kriging interpolation was then performed for the predicted pollutant concentrations for each hourly period. To compare the model results with the observations, the mapped kriging results were cut into hourly sections corresponding to the flight time and location. A mosaic from the hourly sections was assembled to match the flight information. In this manner, a direct comparison between the measured and predicted results can be made and readily observed.

Three dates representing different conditions were chosen for the model validation: July 7, 9, and 17, 2003. In general, the model successfully predicted high O_3 levels for July 7 and July 9 and lower levels on July 17. These predictions were consistent with the flight observations and the synoptic situation that indicated a shallower low pressure system over San Diego on July 17. The model consistently predicted low O_3 concentrations to the east of the Laguna Mountains, an area that due to its topography is not influenced by sources to the west. Further, for all three cases, the model correctly predicted low O_3 over the harbor and downtown areas during the beginning part of the flight period (corresponding to the earliest part of the measurement day). Later in the day, with the flights progressing inland and the air mass aging, O_3 levels were predicted to gradually build up, again consistent with the observations. The buildup terminates as the air masses meet the inland mountain area.

While the spatial and temporal patterns are consistent, the model tended to under predict the observed absolute values. This is a typical problem observed in other studies and is generally corrected by adjusting the inventory to “calibrate” the model. Another possible explanation is the duration of the simulation at each grid cell needs to be extended. Presently the duration of the chemical simulation inside the box model is equal to the residence time of the particle in the box and there is no spin-up period for the chemical reactions. An extension of the time period for the box reactions may address this issue; however, with our current computational resources this is not yet practical.

Local vs. Transported Pollutants

In addition to providing data for model validation, the aircraft sampling results allowed us to assess the impact of local vs. transported pollutants on air quality in the San Diego region. The data from the continuous gas analyzers were translated to image plots that enabled the determination of the impact of the various sources on air quality. The results revealed the following:

- Offshore sources (commercial and military vessels) can be detected through their SO_2 plume.
- The majority of SO_2 in the region is transported from sources south-southeast of San Diego, most likely from Mexico.
- Mobile sources are the main source of precursors leading to the formation of photochemical smog in the region.
- In several cases there is evidence of transport of O_3 and its precursors from sources in the Los Angeles area.

We also found that during most flights, boundary layer (BL) peak levels of O_3 exceeded 100 ppb, and in one case was above 140 ppb.

Model Applications

In addition to developing and validating the hybrid model, we applied the model to two cases relevant to DoD facilities and operations in the San Diego area. The first case involved different emissions scenarios to assess the impact of DoD related emissions on O_3 in the region. It should be noted that the issue of actual impact on a secondary species, such as O_3, is often difficult to discern since it not only depends on the reactivity of the precursor species but O_3 can also be titrated out through the reaction with NO. Thus an increase in NO emissions can lead to an initial decrease in the concentration of O_3 at one point in space and an increase further downwind. Simulations were run for July 11, 13, 19, 21, and 22, 2003 for all sources (civilian and DoD) and the all sources less the DoD contribution. In the absence of DoD emissions, O_3 increased in the region where the sources were previously located (due to the decrease in titration by NO) and increased downwind. The overall contribution of DoD emission sources to the formation or titration of O_3 was found to be between +2% to -12%, depending on location.

Another relevant scenario was to evaluate the impact of emissions from a ship. One of the unique aspects of the hybrid modeling system is the ability to maintain information on emissions from each source in the domain. This enables us to determine the impact of individual sources such as a ship on air quality. The hybrid model enabled us to track the plume over an extended period and assess pollutant transport, dilution, and transformation.

Conclusions

In order to address the impact of emissions in coastal zones, we developed a hybrid model that does not incorporate the chemistry module within the dispersion-advection module but rather implements the chemistry module in a post-processing mode. The hybrid modeling system developed in this study has the following advantages:

- Incorporates the strengths of both the Lagrangian transport/diffusion model and Eulerian multi-box chemical model.
- Modular system that can readily employ alternative chemical and transport-dispersion modules.
- Capable of evaluating impact of emissions from individual sources in space and time (i.e. provides for a source/receptor relationship).

- Designed to evaluate the impact of emissions from moving sources such as ships and aircraft.

As part of this program, we performed an extensive validation of the hybrid model during a period of high O_3 over the San Diego area. This involved a series of aircraft measurements that employed a comprehensive platform for measuring emissions from individual sources and pollutant transport and transformation. We developed a novel approach for using this data to validate the model that will enhance the applicability of future aircraft measurements for testing air quality models. In addition, the database obtained in this phase of the study can be used by other researchers in model evaluation studies.

We also used the model to assess the impact of local and transported pollutants on air quality in the San Diego area and two scenarios of interest to DoD: the impact of DoD emissions on air quality in the San Diego area and the spatial and temporal impact of emissions from a single ship. The major findings from the local vs. transported pollutant component were we could detect emissions from individual sources (i.e., ships) and transported pollutants from Mexico had a major impact on air quality in San Diego. As part of our assessment of the impact of DoD emissions, we evaluated a number of scenarios that included eliminating all DoD emissions in the region. We found this led to both an increase and decrease in O_3 depending on location. This was due to the complex chemistry involved in O_3 formation (i.e., decreasing NO emissions will increase O_3 where the source was removed while increasing it further downwind). Overall, DoD emissions were found to be a small contributor to the levels of O_3 in the region. For the investigation of the impact of emissions from a single ship, we evaluated where its plume traveled and the chemical changes undergone by the emissions from this source. We found the hybrid model was able to resolve the spatial and temporal impacts from a single ship. This type of scenario might be applicable to other cases of interest such as transport of a toxic release in a harbor.

1.0 Objectives

The original Statement of Need (SON) called for the development of improved observational and predictive capabilities to assess the impact of air pollutants emitted as a result of DoD facilities and operations on local and regional air quality. This need was motivated by the fact that many DoD facilities are located in complex environments in and near urban areas that suffer from high levels of ambient air pollution. These operations can be significant sources of O_3 and PM forming precursors, direct PM emissions, and emissions of toxic species. The ability to develop effective predictive tools for these environments, such as coastal zones, has been limited by our inability to faithfully simulate the complex meteorology and chemistry present in these regions.

In order to develop a prognostic modeling system capable of assessing the potential influence of DoD facilities and operations on air quality in coastal zones and applicable to other complex environments, we set out to address the following questions:

- *What is the chemical composition of the emissions and their associated emission rates?* We proposed to account for emission rates of NO_x, SO_2, and PM from ships, PM and NO_x from on-shore diesel activities, and NO_x, CO, speciated hydrocarbons, and PM from other on-shore activities.
- *What is the impact of coastal meteorology on air quality?* To answer this question we modeled the impact of air mass transport and dispersion, coastal thermodynamics and dynamics (surface winds, on-shore/off-shore flow, temperature, and relative humidity), the presence or absence of liquid water, and changes in mixing height on air quality.
- *What is the influence of the land/sea interface on atmospheric chemistry?* The study approach we applied included addressing the contributions from heterogeneous versus homogeneous reaction pathways, appropriate deposition velocities for estimating the fate of the primary and secondary pollutants, and the affect of land/sea interface on photolysis and reaction rate parameters.

In addition, we sought to provide DoD with a methodological approach to answer the following: What are the results of strategies to reduce the impact of emissions from DoD operations on urban scale air quality?

2.0 Background

2.1 Nature of the Problem

One of the most pervasive air quality problems in the U.S. is the high level of urban/regional O_3. Approximately 125 areas in the U.S., containing over 50% of the population, still exceed the O_3 standard, with little immediate prospect of attainment (EPA, 2006). All the major urban areas in California are classified as non-attainment for O_3 (Alexis et al., 2000). Control of O_3 in the troposphere is complicated by the fact that it is a secondary pollutant – it is not directly emitted from sources but is formed through a series of photochemical reactions involving NO_x and VOCs. PM is also a serious environmental issue. In 1999 all but four counties in California failed to meet the state PM_{10} standard (Alexis et al., 2000). While PM_{10} can be secondary in nature, it tends to be dominated by primary emissions, those directly emitted from sources. Recognizing the health impacts of fine particulates (particulates with aerodynamic diameter less than 2.5 μm), the U.S. EPA has implemented new standards for $PM_{2.5}$. Unlike PM_{10}, a significant fraction of ambient $PM_{2.5}$ is produced by secondary reactions.

Many of the urban areas classified as non-attainment for O_3 or PM_{10} and facing non-attainment for $PM_{2.5}$ are located along the east and west coasts and are home to major DoD facilities. These operations can be significant sources of the O_3 and $PM_{2.5}$ forming precursors, direct $PM_{2.5}$ and PM_{10} emissions, and emissions of toxic species. Much of the uncertainty in developing an understanding of the causes of reduced air quality in urban areas is due to uncertainty in the emissions inventories (Seinfeld et al., 1991); however, in coastal areas the situation is confounded by the complex meteorology associated with the land/sea interface. Clearly, there is a need to develop more effective predictive tools if regulatory agencies are to develop effective strategies to reduce air pollution in coastal urban areas.

2.2 Complexity of Meteorology in Coastal Zones

The development of effective predictive tools for environments such as coastal zones is limited, in part, by the inability to faithfully simulate the complex meteorology of the land-sea interface. Meteorological conditions represent a significant determinant of the atmospheric dispersion and chemical transformation of the emitted pollutants. An accurate diagnosis and/or prediction of meteorology is an essential component in understanding the impact of emissions on air quality. In coastal areas with complex topography and marked contrast in surface conditions, large-scale synoptic models experience difficulty in simulating the spatial and temporal detail of the atmosphere necessary for the calculation of the impact of pollutants on, for example, urban areas. Although the modeling system developed in this study can be applied to areas worldwide, in this narrative we focus our discussion on the California coast, which has significant military activities located in large urban areas such as Los Angeles, San Francisco, and San Diego that suffer from air quality problems. The main complexity of the weather on the California coast includes the following:

- Distinct differences between the shallow, cool, stable and moist atmospheric boundary layer over the ocean, which is relatively steady, and the atmospheric boundary over the land with diurnally and synoptically variable characteristics. The understanding and accurate

representation of this discontinuity at the land/sea interface is crucial for reproducing atmospheric, dispersion and chemical processes.

- Seasonally dependent synoptic weather regimes. During the warm season, there is a persistent high-pressure system over the northern Pacific and a low-pressure system over southern California. This creates strong northerly/northwesterly flows offshore along the coast, while the flow regime over the land is much more variable and sensitive to nuances in the synoptic pattern and topographic features. During the cold season, the weather is characterized by the transient frontal systems coming from the eastern Pacific and the Gulf of Alaska. These systems disturb the marine layer (drying, reduced stability, flow regime change) and recovery to a state of equilibrium is seldom achieved during the cool-season (Nov. – March) (Lewis et al. 2003). These conditions become highly relevant for formation and evolution of clouds and fog as shown by Koracin et al. (2001).
- Local circulations in a coastal zone. In the case of relatively weak synoptic forcing, local circulations develop in a coastal zone as a result of differences in heating properties and surface characteristics between the offshore and inland areas. The local circulations are enhanced in the presence of developed coastal topography, sea-surface temperature gradients, ocean currents, and air-sea interaction processes. Even in the case of strong synoptic forcing on the California coast, the local circulations are diurnally influenced by the differences in heating properties over the land and ocean as shown by Koracin et. al. (1998a) and Koracin and Dorman (2001).
- Turbulence structure. The variability in heating, moisture, and wind properties over the land and ocean induces differences in the turbulent fluxes of heat, moisture, and momentum. These fluxes are directly relevant for structure and evolution of transport, dispersion, chemical, and deposition processes of pollutants and tracers over the land and ocean. The understanding and accurate prediction of these turbulence components is crucial for accurate prediction of the impact of pollutants over land and sea.

In view of these complexities, it is easy to understand why the large-scale weather forecast models, with their coarse horizontal and vertical resolutions as well as simple physical parameterizations, have difficulty in accurately predicting the 3D structure of the atmosphere. In recent years, owing to rapid development of computer technology and theoretical work, mesoscale and regional scale models have become an appropriate tool for more accurate prediction of atmospheric conditions in complex terrain environments such as coastal regions. Moreover, a number of operational weather forecast centers are producing continuous real time forecasting (with mesoscale horizontal resolutions of ~10-20 km) for different areas within the U.S. and abroad. These resolutions are significantly better than the 80 – 150 km resolutions typical of the large-scale models. For example, the Naval Postgraduate School (NPS) in Monterey, CA produces MM5 simulations every 12 h with 12 km horizontal resolution grid that cover the California and Oregon coasts. This forecast product provides an excellent source of information for simulation of transport, dispersion, and chemical transformation. Currently, this is the most appropriate forecast for use in this study.

2.3 Limitations of Existing Air Quality Models

In order to assess the impact of emissions in complex environments, an appropriate air quality model is required. Traditionally there are five approaches to the modeling of air quality:

statistical; Gaussian dispersion; single chemical box; Lagrangian; and Eulerian. Each of these models has distinct advantages and disadvantages, which are summarized in Table 1.

Table 1. Advantages and disadvantages of various air quality models.

Type	Examples	Advantages	Disadvantages
Statistical	A) Multivariate statistical	May give highly accurate predictions of daily maximum ozone or particles.	No treatment of physical processes.
	B) Neural nets	Computationally efficient.	Only valid for the current range of conditions.
		Based on historical data.	Cannot be used for air pollution control strategies.
Gaussian Dispersion	Industrial Source Complex - Short Term (ISCST; US EPA))	Simple dynamics.	Cannot be used to model long-range transport over large spatial domains.
		Local predicted concentrations well validated.	Not suitable for modeling reactive tracers or photochemical air pollution.
		Easy to use for "inert" air pollutants.	
		Established for emission permitting purposes.	
Chemical Box	Ozone Isopleth Plotting Program (OZIP; US EPA)	May include highly detailed chemistry.	Treatment of meteorology is highly simplified.
		Algorithmically simple.	Not possible to determine relationship between an emission source and a receptor.
Lagrangian	CALMET/CALPUFF	Physically meaningful air trajectories.	Difficult to account for chemical interactions between different air parcels.
		Very effective in relating emissions from sources to concentrations at receptor sites.	
		May include detailed treatment of chemistry, emission, deposition and other processes.	
Eulerian	Urban Air Shed Model, the Comprehensive Air Quality Model with Extensions (CAM-x)	Allows chemistry and deposition to be treated in more realistic manner.	Spatial resolution is limited.
		Mixing and chemical interactions between different air parcels well described/accounted.	Actual trajectories only indirectly calculated.
			Difficult to relate the emissions from a source to concentrations at a given receptor site.
		May include relatively detailed treatment of chemistry, emission, deposition and other processes.	

Based on the information provided above, no current model was capable of predicting pollutant transport and transformation in complex coastal environments. In order to address this issue, we developed a hybrid model that combines the strengths of Lagrangian models for predicting transport and dispersion and Eulerain models for predicting chemical transformations.

3.0 Methods

In this section the basis behind developing a hybrid air quality model, along with the model components (meteorological driver, Lagrangian particle model, Eulerian chemical model, emissions model, and Lagrangian-Eulerian linkage module) is described. Details of the aircraft platform used to obtain data for model validation are also presented.

3.1 Rationale for the Development of a Hybrid Lagrangian-Eulerian Model

Based upon the limitations of the existing models presented in the previous section, we set out to develop a meteorological air quality model with in-line chemistry that combines the advantages of the Eulerian and Lagrangian models. A Lagrangian model has the advantage that it can more accurately calculate the advection and dispersion from individual sources and allow more complete characterization of the impact of turbulence on the transport of air pollutants. The Eulerian model allows atmospheric chemistry to be treated more realistically and it also allows for the chemical interactions of all air parcels within a grid square (Figure 1).

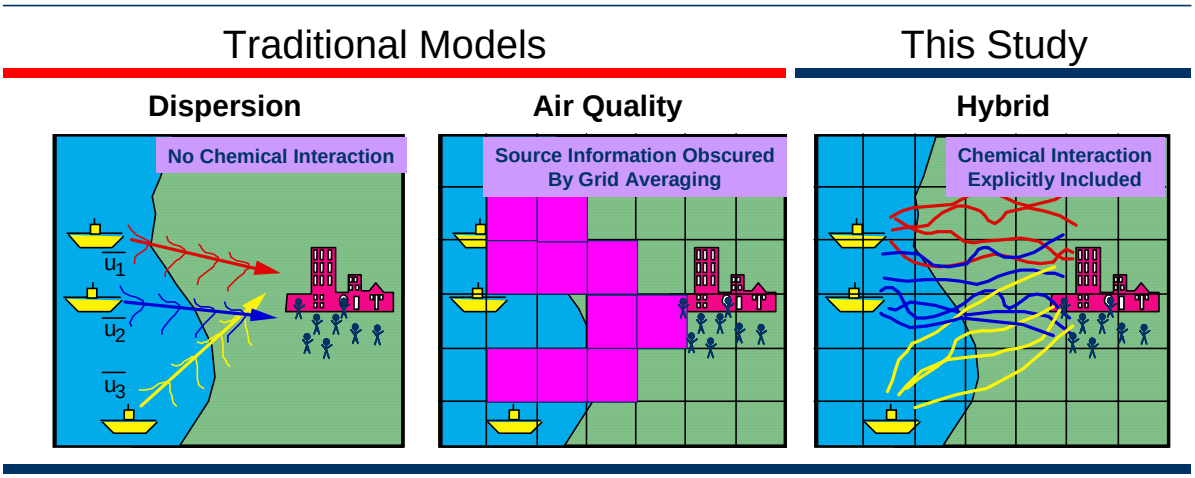

Figure 1. Examples of strengths and weaknesses of traditional modeling techniques and the advantage of the hybrid modeling system.

Consequently the in-line air quality model was divided into two component modules, a Lagrangian random particle module and a chemical module. Advection was done on a Lagrangian basis using the Lagrangian particle model of Koracin et al. (1998b, 1999). This model calculates the transport and advection of Lagrangian particles from emission sources throughout the modeling domain. Besides its three dimensional coordinates, each Lagrangian particle has a unique identification number that will allow its initial source and composition to be determined by the chemical sub-model.

The chemical module places a 3-D Eulerian grid across the modeling domain where the spacing will be commensurate with the particle distribution. The chemical constituents of all Lagrangian particles within each grid square is summed and used to determine ozone and aerosol formation and to estimate the transformation rates of the ozone and aerosol precursors. The chemistry module goes beyond a traditional Eulerian model in that the calculated transformation rates of the ozone and aerosol precursors is used to recalculate the composition of each Lagrangian

particle. This is important because it allows much of source information to be preserved. There are three significant advantages of this hybrid approach. The first is that the advection and dispersion calculation is more accurate than the corresponding calculation in a traditional Eulerian model. The second is that the chemical production of secondary species (e.g., O_3) is more accurate than the production in a traditional Lagrangian model. The third and most significant advance is that the model makes much better estimates of the production of air pollutants from individual emission sources than has been possible with previous approaches.

3.2 Model components

The various components used in the hybrid modeling system are described (Weinroth et al., 2006, Figure 2). These include MM5 for the meteorological fields, a LAP model for advection and dispersion, and a Eulerian chemical model within the Linkage module for the chemical transformations. The Linkage module also couples the Lagrangian and Eulerian parts of the model. One unique aspect of this linkage is that the chemistry model is applied in a post-processing mode (i.e., the LAP model output is used to spatially drive the Eulerian boxes). This allows for flexibility in the use of different model components and significantly lowers the computational requirements. Another key component is the emissions inventory for the region (Kahyaoğlu-Koračin et al., 2006). In addition, the model was evaluated using data gathered during instrumented aircraft flights over the San Diego area between 7 and 25 July 2003.

3.2.1 Meteorological Module

For the meteorological module we used MM5, the Fifth-Generation PSU/NCAR prognostic meso-meteorological model. MM5 is non-hydrostatic, fully compressible, and uses terrain-influenced, vertical sigma-coordinates on a nested horizontal, rectangular staggered-grid. For this study the outer domain was 1125 x 1125 km with a cell size of 15 x 15 km and an inner domain of 275x 305 km with a cell size of 5 x 5 km located over the San Diego area of south western California (Figure 3).

MM5 has been evaluated and applied in a variety of research programs focused on the coastal area of the western U.S. These include studies of (1) atmospheric transport and dispersion of pollutants in the southern California (Luria et al., 2005); (2) atmospheric dynamics, cloudiness, and fog along the California coast (Koračin and Dorman, 2001, Koračin et al., 2005), and (3) the structure and evolution of the winds, wind stress, and wind stress curl impacting ocean dynamics (Koračin et al., 2004).

3.2.2 Transport and Dispersion Module

For the transport and dispersion module we used the LAP model based on the approach described by Pielke (1984). Details of the model structure and applications are described by Isakov et al., (1998) and Koracin et al. (1998a, 1999, 2000). Meteorological input to the LAP model includes 3-D wind and potential temperature fields.

Advection and dispersion calculations are made in a Lagrangian framework. The model uses a volume size (mass/volume) that can be changed to calculate ambient concentrations. Meteorological inputs consisted of the MM5 results. The LAP model uses the same map projection as MM5. The model parameterization includes an option of spatially and temporarily variable or constant time scales, a drift correction term (prevents non physical accumulation of Lagrangian particles during weak-wind conditions), a plume rise algorithm, and three optional

turbulence parameterizations. Emission sources of various geometries including elevated and moving sources with arbitrary time-variable or time limited emission rates can be modeled.

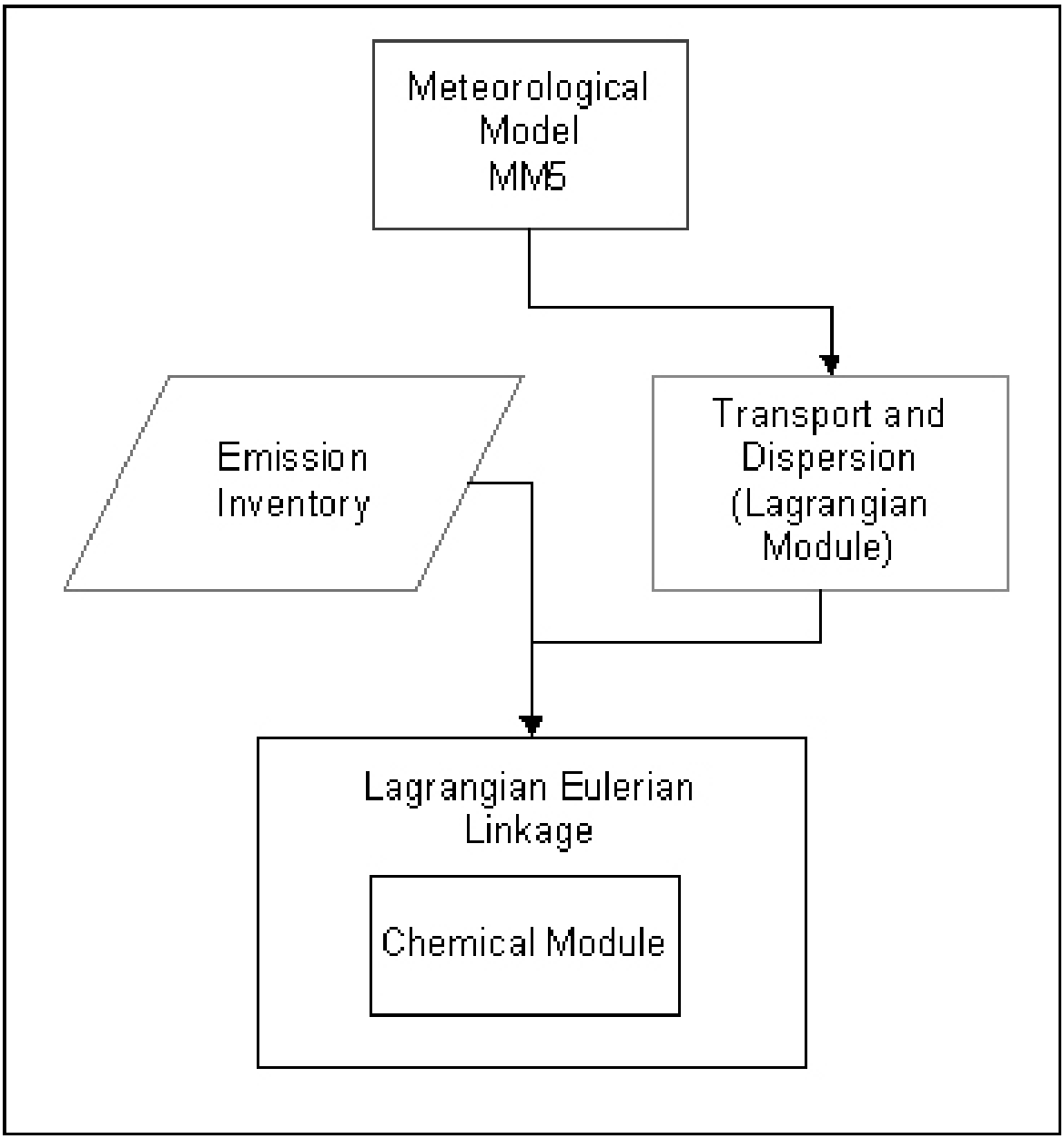

Figure 2. Schematic figure of the modeling system modules. Output from the meteorological module (MM5) is used to drive the transport and dispersion module (LAP). Note the Eulerian chemical model is included in the linkage module.

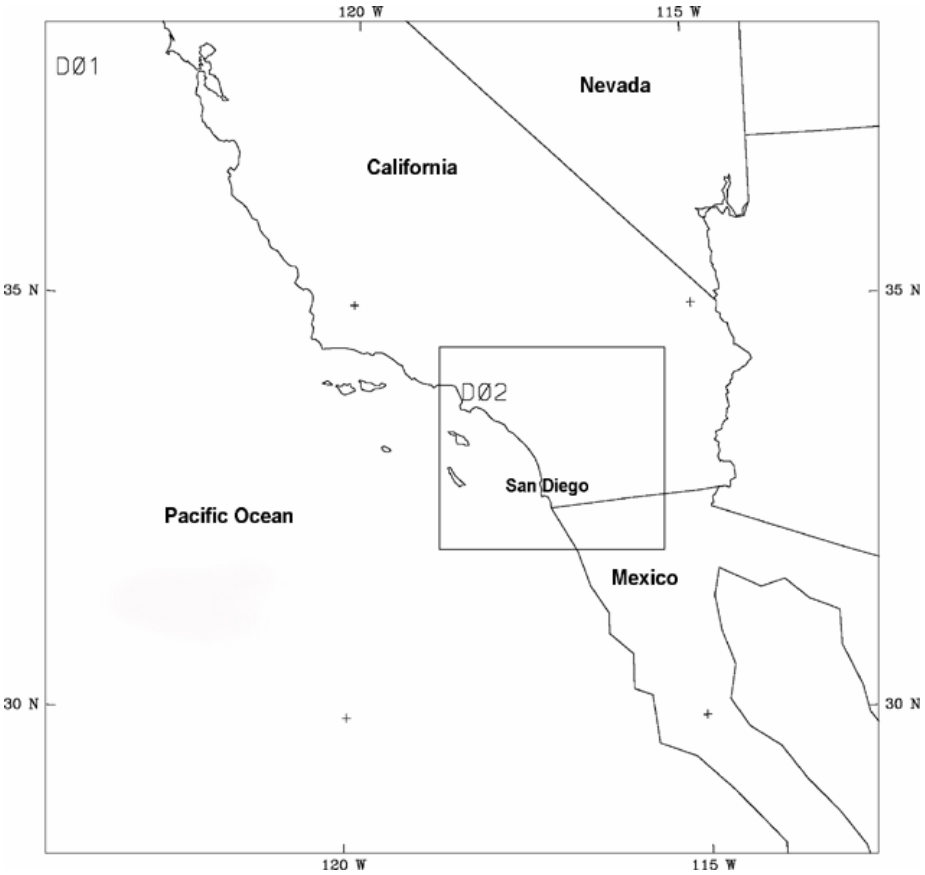

Figure 3. MM5 inner (D02) and outer (D01) domains used in this study. Domains were located over the San Diego area of southwestern California.

3.2.3 Chemistry Module

For the chemical transformation module we used the RACM (Stockwell et al., 1997). The RACM mechanism is a revised version of the RADM2 mechanism (Stockwell et al., 1990), which is widely used in air quality modeling studies. There are a total of 237 reactions in the RACM mechanism. We calculated photolysis rate coefficients for the specific location and time of year according to Madronich (1987).

Simulations were performed using a box model (SBOX, Seefeld, 1997). The chemical compiler reads an input file in which the mechanism's chemical reactions and their rate coefficients are written in a format that is very similar to standard chemical notation.

3.2.4 Lagrangian-Eulerian Linkage

The linkage between the Eulerian and Lagrangian components is based on the concept of a concentration grid cell (Stein et al., 2000). An enhancement was needed for the LAP model to produce a particle specific "name" (ID) for each particle. The identification of the i^{th} particle enables the option to link it to a specific set of attributes (i.e., location, meteorological fields, and chemical composition (j)).

The size of the Eulerian cells can be varied. While very small cells result in homogenous mixing and better spatial resolution of the chemical species, in this study larger cells were used due to computational constraints. We assumed the LAPs had different compositions based on their

original source. A unique feature of this approach is it enabled us to trace any particle at any given time back to its origin and to observe its transformation over time and space.

For each time step and grid cell the particles were disaggregated and the different chemical species were then collected together accordingly (equation 1).

$$P_{total(i\to k,j)t=0} = \sum P_{i,j(i\to k)t=0} \tag{1}$$

Following this, the chemical model was applied. At the end of each time step (1-hr, the same time step as the output from the LAP model), new concentrations within each grid cell were predicted (equation 2).

$$P_{total(i\to k,j)t=1} = RP_{total(i\to k,j)t=0} \tag{2}$$

Apportionment of the chemical concentrations to the individual original particles was made by weighted average (equation 3).

$$P_{(i,j)t=1} = \left(\frac{P_{(i,j)t=0}}{P_{total(i\to k,j)t=0}} \right) P_{total(i\to k,j)t=1} \tag{3}$$

Distribution of newly produced chemical species was based on the diffusion time scale, mixing height, and turbulence intensity (equations 4 – 7). An empirical number was calculated using the approach outlined by Song et al., (2003). For our study this factor (fac) is 0.05.

$$P_{total(i\to k,j)t=1} > P_{total(i\to k,j)t=0} \tag{4}$$

$$P_{(i,j)t=0} = 0 \to P_{(i,j)t=1} = \frac{B_{(j)} * fac}{N_0} \tag{5}$$

where N_0 = number of particles where specific chemical are equal to zero and

$$B = P_{total(i\to k,j)t=1} - P_{total(i\to k,j)t=0} \tag{6}$$

For particles where the specific chemical species concentrations are non-zero, then

$$P_{(i,j)t=0} > 0 \to P_{(i,j)t=1} = \left(\frac{P_{(i,j)t=0}}{P_{total(i\to k,j)t=0}} \right) \left(p_{total(i\to k,j)t=1} - \left(B_{(j)} * fac \right) \right) \tag{7}$$

This is shown schematically in Figures 4a-c. As shown in the figure, each particle has an individual identity denoted by different symbols. This identity contains both source and composition information. Two layers (each 1 km in height) from the box model are shown in Figure 4a. Most particles are located in the lowest level, which represents the mixed layer. In Figure 4b the map of the study area can be seen in low resolution, with the grid surrounding the San Diego metropolitan area. Gray dots represent clusters of particles. When we zoom in (Fig. 4c), we can see the box model cells (15 x 15 km), along with the MM5 inner grid cells (5 x 5 km). In the example, 11 particles are shown but the model can handle up to 20,000 particles per grid cell. After each time step the species are redistributed (equations 1-7) and new particle positions are calculated by the LAP model.

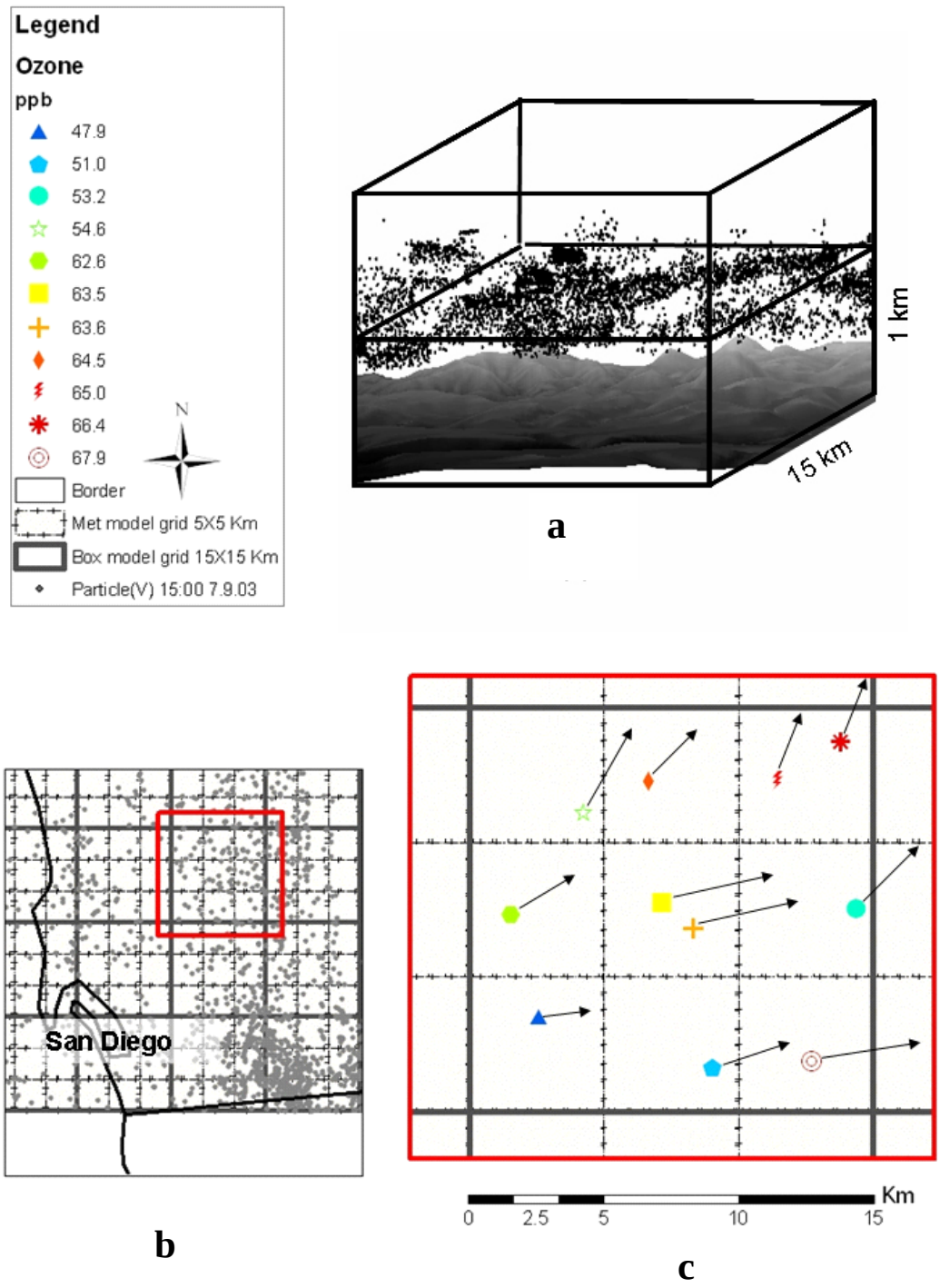

Figure 4. Schematic showing the main features of the Lagrangian – Eulerian linkage. (a) Results from 2 levels of the LAP. (b) Bird's-eye view of the Eulerian grid above the study area. (c) Enlargement of Eulerian cell superimposed on the meteorological model inner grid. Particles shown in (c) have different composition as denoted by the different symbols. Arrows are grid specific vectors of wind speed and direction.

3.2.5 Emission Inventory

In this study we used the emission inventory developed by Kahyaoğlu-Koračin et al., (2004; 2006). This was based on the Southern California Oxidant study (SCOS) 1997 day-specific emissions inventory and the California Air Resources Board (CARB) annual inventory. The inventory domain contained 110 x 74 grid cells of 5 x 5 km. Species included NO_x, SO_x, CO, PM, and TOG for all sources, including on-road and off-road mobile sources, industrial sources, commercial and U.S. Navy marine vessels, and commercial, civil, and military aircrafts. Note, the military component of the inventory makes up only a small percentage of the totals for all species (Figure 5). The biogenic component of the inventory was recalculated for the validation period using observed temperatures and day-specific solar radiation values.

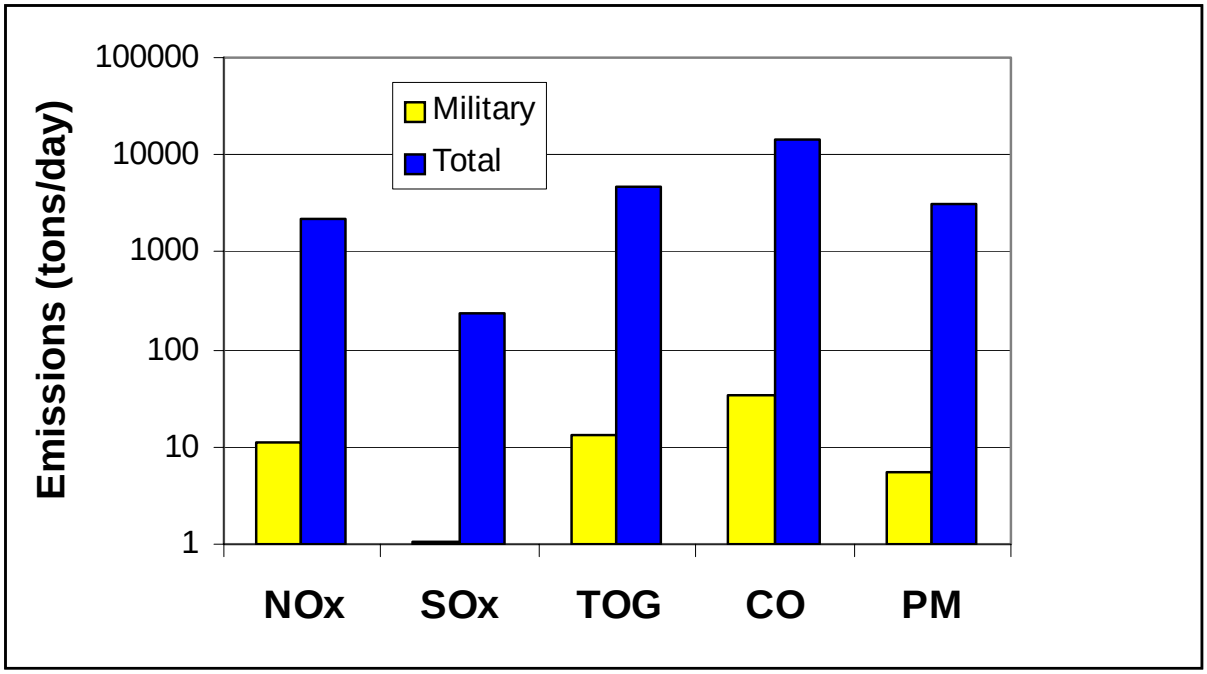

Figure 5 Emissions from DoD activities in San Diego vs. the total inventory.

3.3 Airborne Measurements for Model Validation

In order to obtain data to validate the modeling system, an airborne sampling study was conducted in the San Diego area during July 2003 (Luria et al., 2005). A description of the measurements are presented below.

Samples were collected using an instrumentation package operated aboard a twin engine Twin Otter aircraft (Figure 6). Except for the CO instrument, the gas analyzers on board were all manufactured by Thermo Environmental Instruments Inc., Franklin, MA (TEII). Instruments included a Model 43S SO_2 analyzer and several other Model 42 and 42S TEII analyzers that were modified to directly measure NO, NO_2, NO_y, NO_z^* (= NO_y after sampling through a nylon filter to remove nitrates, see Tanner et al., 1998) and O_3. By adding or taking the difference of signals from these analyzers, the levels of NO_x, NO_z and nitrate could be determined. CO was measured with a Aero-Laser Model AL5002 vacuum UV fluorescence instrument with 1-s response time. Other continuous measurements included location, pressure (altitude), temperature, humidity and particle light scattering. The data from all continuous monitors were

recorded at 1s and 5s intervals. The 1s data were used for the calculated parameters, whereas the data analysis was performed on the 5s data set. The response time of the gas analyzers was less than 5s for 90% of the signal. The sampling air speed was 180 km h^{-1}, thus, the special resolution of the data is approximately 0.25km. Additional information on the instruments and their mode of operation is given in Table 2. Figure 7 shows the arrangement of the instruments on board the aircraft. Further details regarding the instruments, their performance, the sampling manifold, calibration procedures and the data system are given in previous publications (Valente et al., 1998; Luria et al., 1999 and Luria et al., 2000).

Figure 6. Twin Otter aircraft taking off from El Cajon.

Altogether five preliminary and ten research flights were performed. The flights took off from Gillespie airfield near Santee township, located some 25 km north-east of downtown San Diego. The first segment of the flight consisted of ascent to 6000' (1830 m) above sea level (ASL) and a constant-level flight in the free troposphere (FT) to a 'way point' over the water, just west of the San Diego Harbor. Over this point the aircraft spiraled down to an elevation of 300m ASL. The 'way point' was the center of a series of 9-11 concentric arcs taken at a 3-8 km interval, inside the BL at an altitude of approximately 300m above the surface. Over the low land and near the coast, the aircraft maintained constant elevation. Over the mountainous region frequent changes in altitude were necessary in order to follow the terrain features. At the end of the last arc the aircraft climbed back to 6000' ASL for the last 15 minutes of the flight and then spiraled down over the airport before landing. The duration of each flight was approximately 5 hours of which

~4 hours were inside the boundary layer. A typical flight track (Flight 8) is illustrated in Figure 8 over a geographical map of San Diego County.

Table 2. List of real time measurements performed on board the aircraft.

Instrument	Maker/Model	Principal of operation sensitivity	Modification/ analysis method	Parameter to be measured
NO_x Monitor	TEI model 42S	Chemiluminescence 0.1 ppb	No converter	NO
NO_x Monitor	TEI model 42S	Chemiluminescence 0.1 ppb	Xe lamp converter (NOAA/ARL modified)	NO_2 (measured as $NO+NO_2$)
NO_x Monitor	TEI model 42S	Chemiluminescence 0.1 ppb	CO on heated gold catalyst	NO_y
NO_x Monitor	TEI model 42S	Chemiluminescence 0.1 ppb	CO on heated gold catalyst plus Nylon filter	Particle NO_3^- + HNO_3 (measured as NO_y-NO_y^*)
NO_x Monitor	TEI model 42S	Chemiluminescence 0.1 ppb	Operated in reversed mode for fast response	O_3
O_3 Monitor	TEI model 49	Light absorption 0.5 ppb	Standard configuration	O_3[1]
SO_2 Monitor	TEI model 43S	Pulsed fluorescence 0.1 ppb	Standard configuration	SO_2
CO Monitor	Aero-Laser GmbH Model AL 5002	Laser-induced UV fluorescence 0.2ppb	Standard configuration	CO
3λ - Nephelometer	TSI Model 3560	Optical scattering of particles	Standard configuration	Light scattering coefficient
Temperature and Humidity	Custom built	0.1°C, 1%		T & RH
Location		GPS 50m		Longitude, Latitude
Heading		Magnetic Compass 2°		
Wind Speed and Direction	Aventech CAN Model AIMMS20	GPS&Compass 1m/s, 10°		WDD, WDS
Pressure/Altitude	Custom built	0.2 mb		P, Alt

[1] For calibrations only, performed at the base of operations.

Figure 7. Setup of instruments on board the aircraft. The hanging bag is for collection of the carbonyl samples prior to trapping with cartridges.

Table 3 lists the 10 research flights, their duration, and the extent to which data from the various measurements are available. For each flight, the data from all continuous monitors were used to construct image plots that interpolated the data over the geographical domain. The interpolation was done by the Kriging method using commercial software (Surfer by Golden Software, Golden, CO). Since the prevailing winds were from the west and since the aircraft moved eastward at a rate that was comparable with the mean wind speed (15-25 km h^{-1}), the image plots (see Figure 9) approximately represent the chemical composition of an air mass in an approximately Lagrangian fashion as it travels inland from the coast.

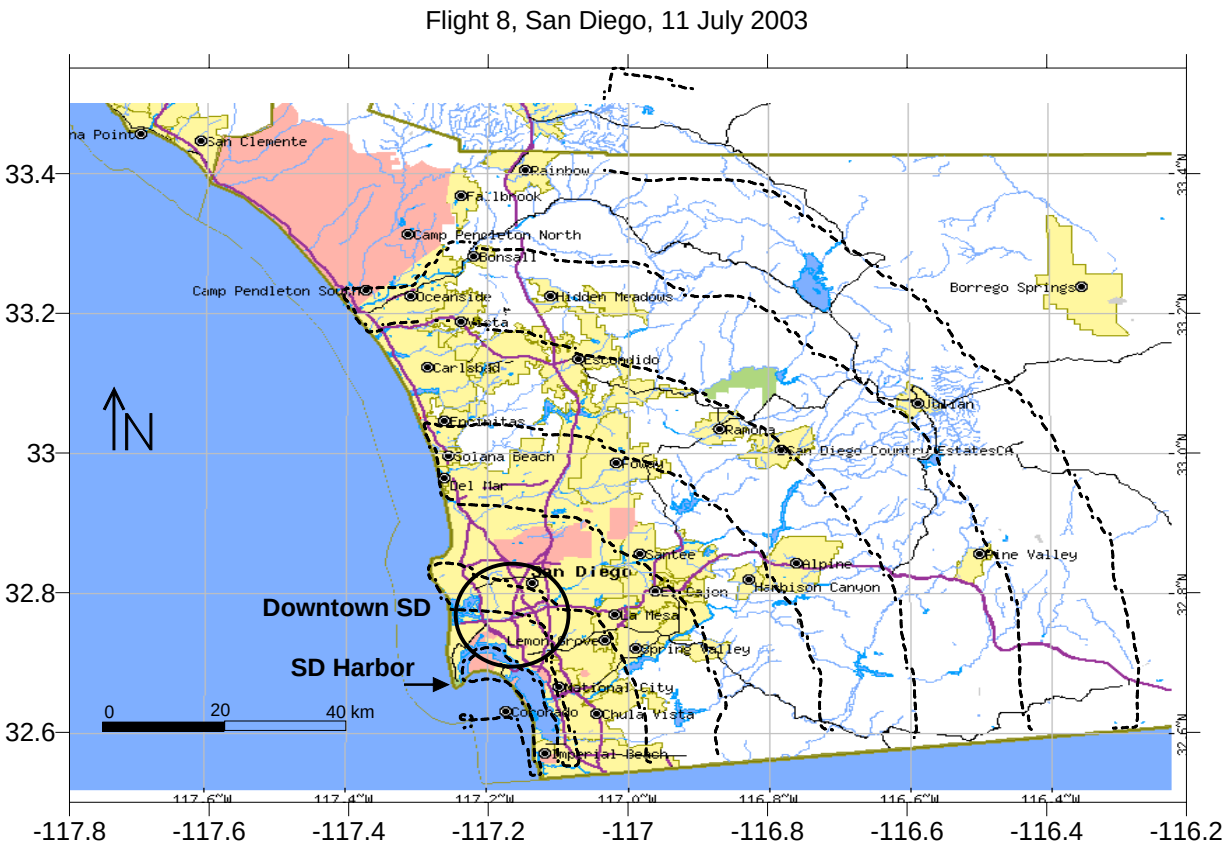

Figure 8. The tracks of Flight 8 (11 July) presented over a map of San Diego and vicinity.

Table 3. Summary of San Diego Flights – July 2003.

FLIGHT Number,	Date	Flight Start-End (Dec. Hours)	Low Level Start-End (Dec. Hours)	Data Available
Ft 6	7/7/2003	11.42-16.58	11.78-15.87	All, some CO data missing
Ft 7	7/9/2003	12.28-17.71	12.81-17.00	All
Ft 8	7/11/2003	11.51-17.06	11.99-1620	All
Ft 9	7/13/2003	11.43-16.86	11.83-16.30	All
Ft 10	7/17/2003	11.58-16.93	12.16-16.50	All, limited wind data
Ft 11	7/19/2003	11.50-16.64	12.17-16.12	All
Ft 12	7/21/2003	11.30-16.53	11.84-16.00	All
Ft 13	7/22/2003	11.39-15.64	12.00-15.14	All
Ft 14	7/24/2003	11.42-16.88	11.93-16.34	All
Ft 15	7/25/2003	11.33-16.79	11.88-16.22	All

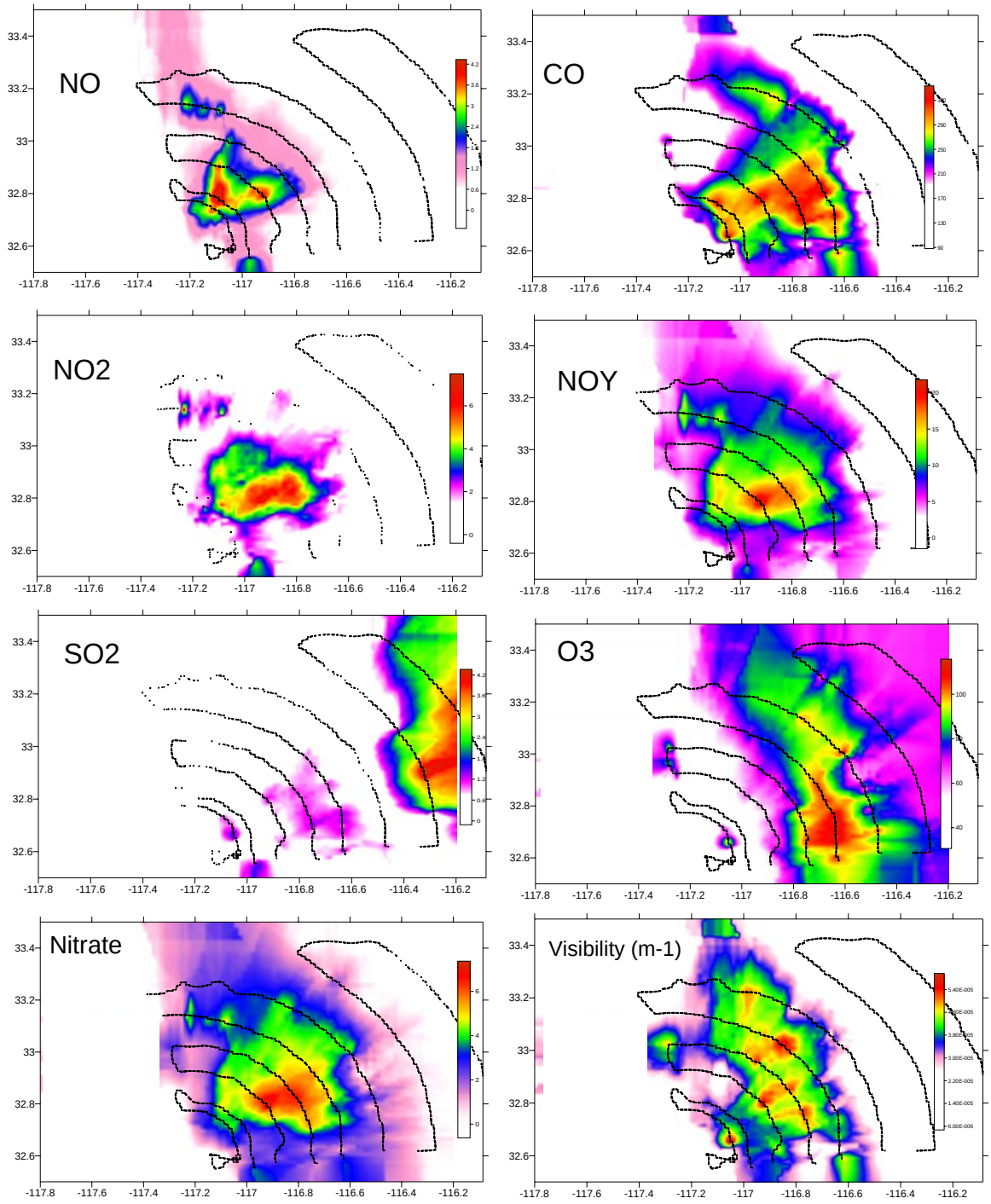

Figure 9. Image plots of NO, CO, NO_Y, Ozone, SO_2 and visibility. All plots are taken from Flight 7 (9 July).

4.0 Results and Accomplishments

In this section are described the application of the aircraft measurements for model validation and an assessment of local vs. transported pollutants in the San Diego area. In addition, we discuss two applications of the hybrid model: (1) assessment of DoD emission on air quality in San Diego and (2) the impact on air quality of emissions from a single ship.

4.1 Model Validation: Comparison between Observations and Predictions

Three dates representing periods of elevated O_3 were chosen to validate the model: July 7, 9, and 17, 2003. These were characterized by a low pressure system over the north tip of the Gulf of California with a local trough extending towards the Baja Peninsula. High pressure zones prevailed over the Pacific Ocean and inland regions of California and Arizona. In general, the local sea-land breezes were the major factor affecting local pollutant dispersion and transport between the coast and the Laguna Mountains. East of the mountains, the prevailing flow was from the southeast. During the validation period, the center of the low was deeper on July 7th and became more shallow for the other dates. During the latter two dates, a strengthening high pressure system to the east coupled with the high over the ocean tended to force the low pressure system to the south.

Examples of model results versus airborne measurements can be seen in Figures 10 – 12. The flight path is shown as the colored dots, which also represent the observed ozone concentration. Modeled ozone concentrations were calculated for each particle during each hour of the flight period. A kriging interpolation was performed for the predicted ozone concentrations for each hourly period. One issue was how to compare the hourly model predictions with the continuous aircraft measurements. To make this comparison, the mapped Kriging results were cut into hourly sections corresponding to the flight time and location. A mosaic from the hourly sections was assembled to match the flight information (hourly results that were assembled to produce the mosaics are contained in the lower sections of Figures 10 -12). In this manner, a direct comparison between the measured and predicted results could be made and readily observed.

For July 7 (Figure 10), four Kriging interpolation segments were combined to cover the time period from 1200 to 1600 LST. Good agreement between the model results and the fight observations is seen in the figure. For the 1200 to 1300 segment, the model predicts low O_3 levels (40 - 60 ppb) similar to that seen in the airborne observations. The small regional O_3 peak at observed in the center of the figure is also well predicted. O_3 is underpredicted towards the south east section (lower right corner) but is well reproduced later along the flight track.

On July 9 (Figure 11) reasonable agreement is recorded between the model and measured ozone concentrations. During the beginning part of the flight path two high concentration levels are seen in the harbor and slightly inland. The model does not capture these hotspots, likely due to the coarse resolution of the inventory. For the 1300 to 1400 period, lower levels are seen slightly inland from the downtown area, consistent with the model predictions. Over the next two hours (1400 – 1600 LST) the model predicts elevated levels inland toward the mountains, as seen in the aircraft observations; although, an overprediction is observed in the northwest corner of the region (near Camp Pendleton).

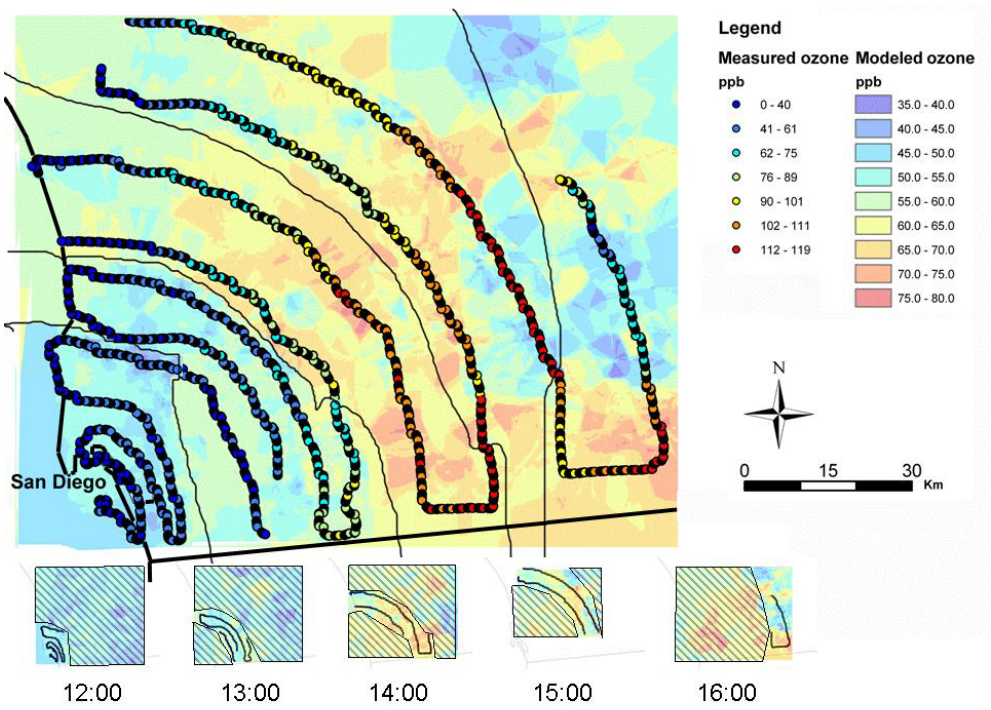

Figure 10. Comparison of observed vs. predicted ozone concentrations for July 7, 2003 1200-1600.

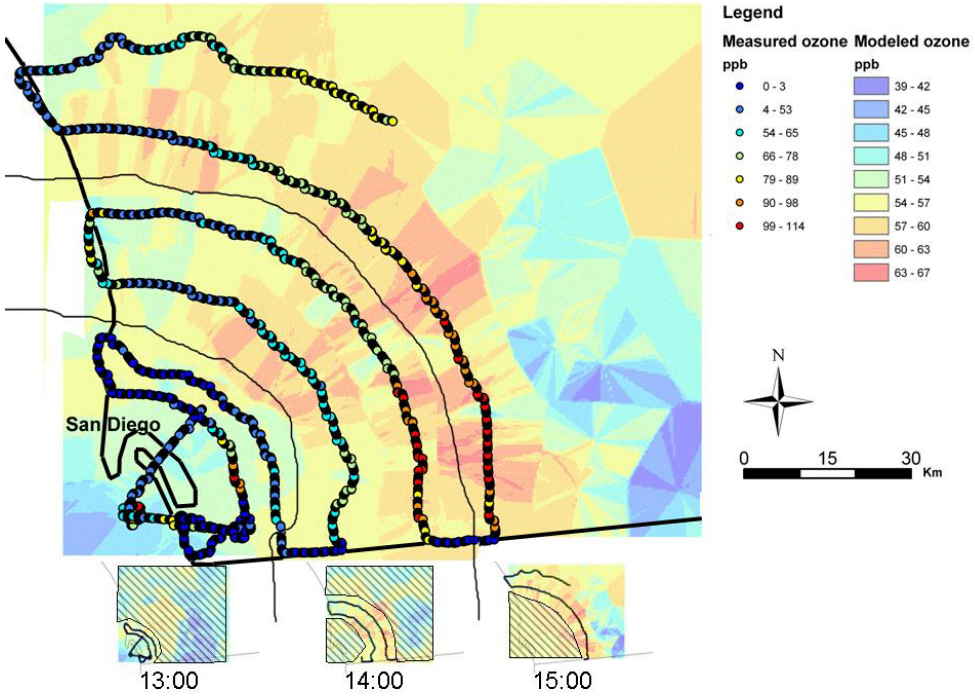

Figure 11. Comparison of observed vs. predicted O_3 concentrations for July 9, 2003 1300-1500.

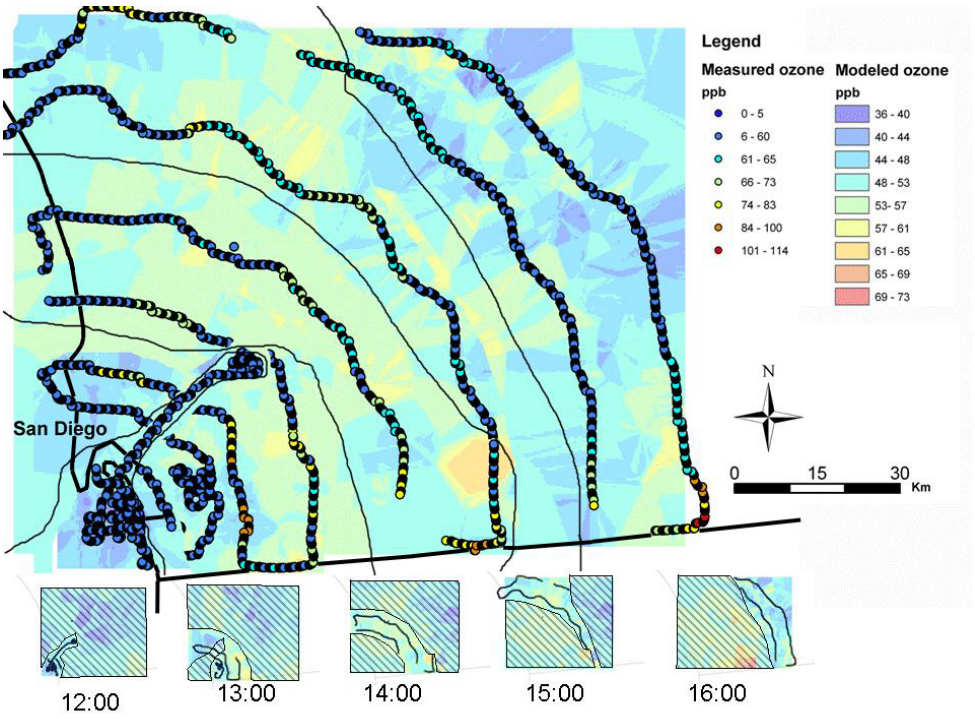

Figure 12. Comparison of observed vs. predicted O_3 concentrations for July 17, 2003 1200-1600.

In the last example (July 17, Figure 12), aside from localized hotspots, the predictions and observations have good spatial and temporal agreement. During the early period the model and measurements agree on the location of the ozone trough over the San Diego metropolitan area. Later in the day, generally uniform levels of ozone reside over the most of the study area (except for the border with Mexico), as seen in the measurements.

In general, the model successfully predicted high O_3 levels for July 7 and July 9 and lower levels on July 17. These predictions are consistent with the flight observations and the synoptic situation that indicated a shallower low pressure system over San Diego on July 17. The model consistently predicted low O_3 concentrations to the east of the Laguna Mountains, an area that due to its topography is not influenced by sources to the west. Further, for all three cases, the model correctly predicted low O_3 over the harbor and downtown areas during the beginning part of the flight period (corresponding to the earliest part of the measurement day). Later in the day, with the flights progressing inland and the air mass aging, O_3 levels were predicted to gradually build up, again consistent with the observations. The buildup terminates as the air masses meet the inland mountain area.

While the spatial and temporal patterns are consistent, the model tended to underpredict the observed absolute values. Measurements ranged between of background of approximately 40 ppb up to a maximum of nearly 120 ppb. Model predictions did not exceed 80 ppb. This is typical problem observed in other studies (Bauer and Langmann, 2002, Biswas and Rao, 2001, Rao and Sistla, 1993, Sillman et al., 1998, Tory et al., 2004) and is generally corrected by adjusting the inventory to "calibrate" the model. Alternatively, this may be due to overestimating the turbulence transfer. Future turbulence measurements are needed to address

this issue. Another possible explanation is the duration of the simulation at each grid cell needs to be extended. Presently, the duration of the chemical simulation inside the box model is equal to the residence time of the particle in the box and there is no spin-up period for the chemical reactions. An extension of the time period for the box reactions may address this issue; however, with our current computational resources this is not yet practical.

4.2 Local and Transported Pollutants Over San Diego

In addition to providing data for model validation, the results of the airborne study enabled us to assess the impact of local and transported pollutants on air quality in the San Diego area. Details of these results are contained in Luria et al. (2004) and are briefly described in the sections that follow.

4.2.1 Air Quality Measurement Results

Nitric Oxide: NO is the best indicator for fresh emissions from all combustion sources. Since mobile sources are the dominant source of NO (and NO_2 rapidly derived there from) emissions, the observed levels can be attributed to these sources. In all 10 flights the signature of downtown traffic emissions is evident. No distinct NO signature from the offshore sources was observed along the coastline. Peak NO levels measured in the well-mixed BL were up to 10 ppb, and they decreased rapidly to below 1 ppb by the time the downtown plume reached 15-20 km from downtown.

Carbon Monoxide: Like NO, CO is also an indication of fresh emissions, almost exclusively from gasoline powered motor vehicles. Unlike NO, CO has a very long atmospheric lifetime (on the order of one month). Thus, it is expected that if both NO and CO have a common source, their relative plume concentration images will be similar, but with the CO plume being broader. This results from the fact that its concentrations decrease as the air mass travels downwind only by dilution, whereas [NO] decreases also by conversion to other NO_Y species. During the study, CO levels in the well mixed BL peaked at 0.5 – 0.7 ppm and decreased to below 0.2 ppm at the edges of the study domain.

Total Nitrogen Oxides (NO_Y): While NO_Y is a surrogate for all combustion sources, a comparison between the NO_Y and the CO images for all 10 flights shows a close similarity, an indication of a common dominant source (i.e., motor vehicles). The fact that NO_Y plume images coincide more closely to the CO images than do the NO images is expected, since the atmospheric lifetime of the entire NO_Y group is substantially longer than that of NO alone. NO_Y levels in the BL maximized at ~30 ppb, usually over downtown, and dropped to below 4 ppb at the edges of the research domain.

Ozone: Peak O_3 levels observed during this study were in fact higher than those observed at any of the ground monitoring stations. This is expected since O_3 is removed by dry deposition near the surface (Van Valin et al., 1994). In most cases the highest O_3 levels were detected within the domain, with lower levels at the edges. This observation is consistent with processes dominated by local sources. However, in a few cases there were indications that the elevated O_3 levels resulted from transport of sources north of the region (see Table 4). The differentiation between local and transported sources is based on the wind direction, the location of the O_3 cloud plume, and the relationship between the NO_Y and O_3 plumes. Table 4 summarizes the O_3 information from all 10 flights. The highest values observed at the air monitoring site on the ground were at

the San Diego Alpine air quality monitoring site on July 5 and 8, 2003, with a 1-h max value on both days of 108 ppb (California Air Resources Board, 2004).

Sulfur Dioxide: Because of strict emission controls, SO_2 emissions in California are very low. It was assumed that the SO_2 traces from offshore sources could be used to identify them. Indeed, during several flights SO_2 emissions which originated in the vicinity of the San Diego Harbor were detected as the air mass drifted eastward. During at least half of the research flights with peak values of up to 5 ppb. Background levels were significantly lower, usually below 0.4 ppb. Unlike other spatially correlated pollution images discussed earlier, the SO_2 images were quite different. During half of the flights, high levels of SO_2 were measured over a wide area at the eastern edge of the domain. These relatively high levels were not accompanied by elevated levels of any other pollutant.

Table 4. Summary of peak O_3 values observed during the flights.

Flight	**Peak O_3, ppb**	**Probable source**
Ft 6	120	Local
Ft 7	135	Local
Ft 8	141	Local and transport of O_3 from the north
Ft 9	135	Local
Ft 10	133	Local and transport of O_3 from the north
Ft 11	88	Local
Ft 12	105	Local
Ft 13	112	Local
Ft 14	104	Local and transport of O_3 from the north
Ft 15	104	Local

Visibility: The only means available for estimating particle levels in this study was a TSI Model 3560 3-λ light scattering instrument. The image plots of the light scattered in the green wavelength's region showed that visibility over most of the region was good (light scattering < $1x10^{-5}$ m^{-1}, i.e., < 10 Mm^{-1}). The light scattering image was similar in many ways to the nitrate image, suggesting that particulate nitrate is a main component of the particulate load. Furthermore, the lack of any correlation between light scattering and SO_2 at the eastern edge of the domain suggests that the SO_2 cloud plume observed is rather fresh and that significant conversion to particulate sulfate has not yet occurred.

4.2.2 Sources of Photochemical Smog in San Diego

The evolution of photochemical smog in the San Diego downtown plume is demonstrated in Figure 13 for Flight 11. As shown, there is one distinct source of NO over the downtown area (Fig. 13a). The NO plume is very short lived and rapidly converts to more extensive NO_2 and NO_Y plumes (Fig. 13b and 13c). The CO trace (not shown) is again very similar to that of the NO_Y. The conversion of reactive NO_Y species (NO_X=NO+NO_2) to less reactive species (nitrate, nitric acid and PANs) occurs quite rapidly as can be seen from the nitrate image on Figure13d when compared with that of the entire "odd nitrogen" group (NO_Y, Fig. 13c).

The conversion of NO_X to NO_Z (NO_Z=NO_Y-NO_X) is illustrated in Figure 13e, which shows the so-called "chemical age" (NO_Z/NO_Y) of the nitrogen plume (Trainer et al., 1993). Low chemical ages (<0.4) are indicative of fresh emissions while high values (>0.7) indicate that the photochemical processes producing NO_z are nearly complete, and little or no new additional O_3 can be produced (Olszyna et al 1994). Figure 13e shows that the reactive zone is confined to near the downtown area and it becomes less reactive as the plume travels to the northeast. Consequently, when the chemical age increases to above 0.7, O_3 is formed as the air mass ages and reaches its peak level where the chemical age approaches 0.8 (Figure 13f).

4.2.3 Pollutant Transport

The phenomenon of an isolated SO_2-rich region, observed in at least 5 of the 10 flights, was most evident on Flight 9. Over this area (an isolated 'island', inland east of 116.5ºC W longitude) SO_2 levels exceed 4 ppbv, significantly higher than those observed over the rest of the domain. The latter were typically below 0.5 ppbv, except for a small area covered in plumes from the coastal sources. The area over which elevated SO_2 levels was observed is defined by very sharp borders, as determined not only from the SO_2 image but also by three other independent measurements - wind direction, O_3 and CO. Because of the location, the wind direction and the high ratio, it is highly unlikely that the source for this polluted air is from within the U.S. This source likely originates from a metal refining operation or similar smelter-type source with limited or no pollution controls located across the border in Mexico.

The data from Flight 9 seem to show that the region can be affected not only by transport from Mexico but also by sources north of the domain (i.e., Los Angeles). In all other flights the highest CO levels were observed in the vicinity of the fresh NO emissions. On Flight 9 the highest CO concentrations were not associated with fresh emissions but were co-located with an O_3 peak with high chemical age (NO_Z/NO_Y> 0.8). In this specific case, it is unlikely that the source of the emissions was downtown San Diego, and that even after travel times of several hours the CO levels were still higher than those observed over the traffic sources near downtown. The only feasible explanation is that the air in this region has mixed with another air mass originating north of the domain. Onboard in situ wind measurement indicates that the airflow at this location is from the north-northwest direction, which may suggest transport from the Los Angeles metropolitan area.

4.2.4 Impact of Local and Transported Pollutants

Based on the results presented in this section, the conclusions of this component of the study are as follows:

- Offshore sources (commercial and military vessels) can be detected through their SO_2 plume which is easily identified due to the low SO_2 regional background
- The majority of SO_2 in the region is transported from sources south-southeast of San Diego, most likely from Mexico. The ratio of SO_2/NO_Y suggests emissions are from sources with limited or no controls.
- Vehicular transportation is the main source of precursors leading to the formation of photochemical smog in the region. During most flights it was observed that the entire process of daytime conversion of the fresh NO emissions leading to the formation of

ozone and NO_z (HNO_3, nitrate and PANs) occurred over the metropolitan area within the domain of this study.

- In several cases there is evidence of transport of O_3 and its precursors from sources in the Los Angeles area.

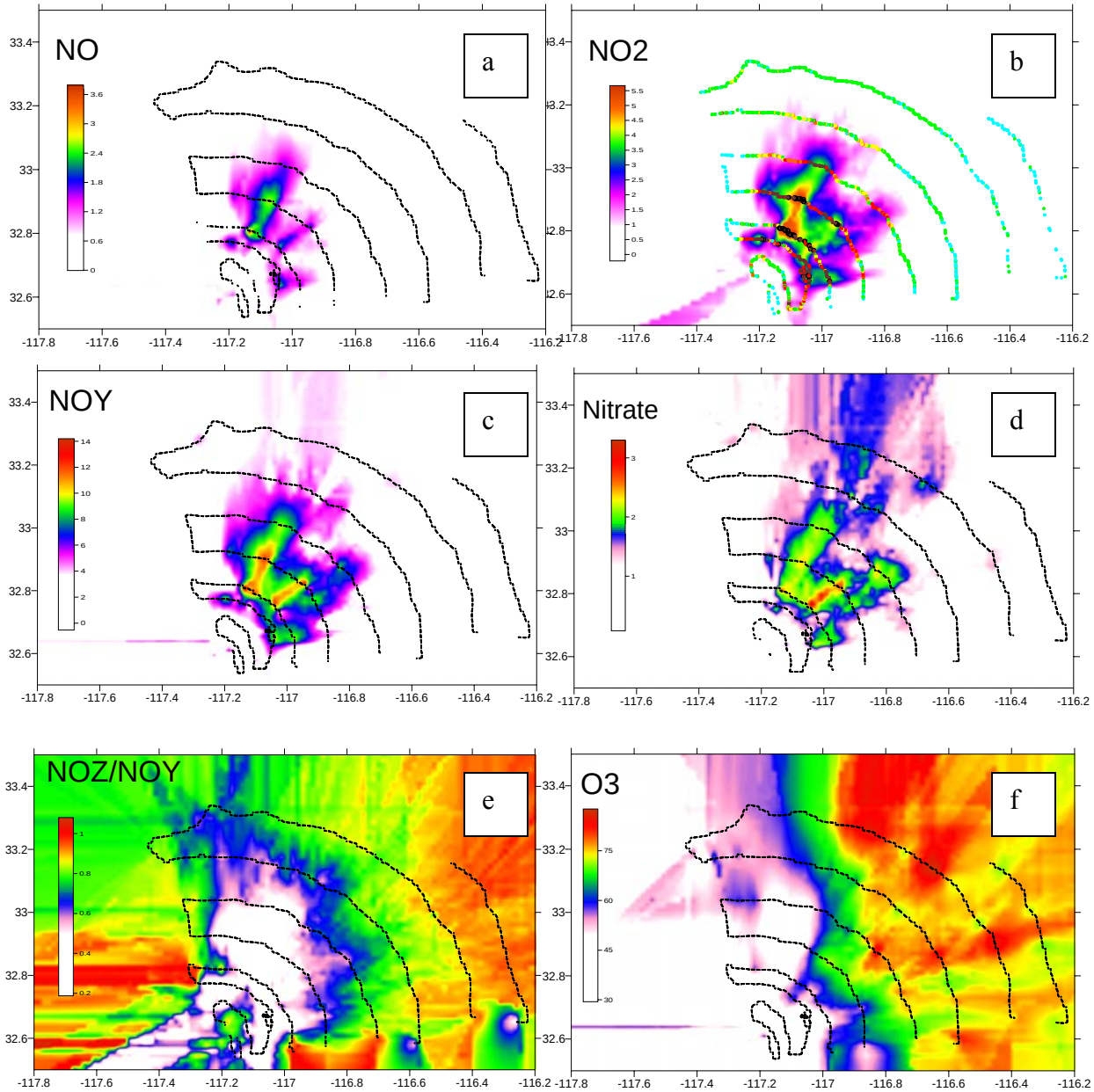

Figure 13. Image plots of NO, NO_2, NO_Y, nitrate NO_Z/NO_Y and O_3 calculated from the measurements performed on 19 July (Flight 11).

4.3 Impact of Emissions from DoD Activities on Air Quality in the San Diego Area

As discussed in the introduction, DoD training and operational activities are a source of pollutant emissions that can impact air quality. A number of previous studies have sought to address this

issue. For example, Odman and Russell (2002) used two techniques to assess and analyze the impact of Fort Benning, GA, on the neighboring Columbus metropolitan area: an adaptive grid, that dynamically reduces the grid size to better resolve evolution of the plumes from the source to the receptor coupled with direct sensitivity analysis, that efficiently yields the sensitivity of pollutant levels to emissions from various sources. As part of a risk assessment study looking at populations living near large airports (analogous to some DoD facilities), Tesseraux (2004) used available monitoring data and found that there is an impact on the air quality of the adjacent communities but this impact did not result in levels higher than those in a typical urban environment. Corbett and Koehler (2003) investigated the contribution of ship emission to an overall emissions inventory and concluded that global NO_x emissions more than doubled. This work also produced a detailed sensitivity analysis of the inputs to these estimates, identifying uncertainty in vessel duty-cycle as critical to overall emissions estimates. While the Odman and Russell (2002) work focused specifically on the impact of DoD emissions, none of these studies considered the impact of coastal emissions on urban air quality.

In order to address this issue of impact assessment, a series of model runs were performed varying the emissions from DoD related sources for the intensive monitoring period used in the validation component of this work (July 2003). The issue of actual impact on a secondary species, such as O_3, is often difficult to discern since it not only depends on the reactivity of the precursor species but can also be titrated out through the reaction with NO. Thus an increase in NO emissions can lead to an initial decrease in the concentration of O_3 at one point in space and an increase further downwind.

Figure 14a shows the model predicted O_3 at 1600 on July 19, 2003 for all emission sources. We see that the area north of San Diego has elevated O_3 levels of up to 70 ppb. This is primarily attributed to the emissions originating in Los Angeles. The long ridge of ozone in the north east part of Figure 14a is due to polluted air from San Diego area that has undergone chemical reactions to form additional O_3. In Figure 14b the model shows the results when all DoD emissions were removed from the inventory. The main spatial features of the O_3 distribution is similar to that shown in Figure 14a. The difference between the two scenarios is shown in Figure 14c. This indicates that the added emissions from coastal DoD operations titrates out the O_3 near to the sources, as demonstrated by the two large blue areas of decreased ozone levels (-11 and -5 ppb) in the south part of the domain. There is a negligible increase, up to 2 ppb) in other regions. It should be noted that the area being affected by the titration of O_3 due to emissions from DoD operations is quite large (8000 km^2).

Simulations were also run for July 11, 13, 21, and 22, 2003 to further investigate the impact of emissions from DoD sources. The difference graphs (similar to 10c) for these four scenarios is shown in Figure 15. In Figure 15a we observe an increase in the O_3 concentration in the northern part of the city. Further north of this small ridge (2 ppbv), we find a decrease in O_3 of up to 6ppb (i.e., without DoD emissions, O_3 is reduced by 6ppb). This period is unusual when compared with the other simulation dates in that the wind is predominately northerly; leading to transport of emissions from the south. In Figure 15b we see alternating increases and decreases in the O_3 levels following removal of the DoD emissions. This behavior is due to the ratio sensitivity between the precursors of O_3 (NO_x and VOCs). For July 21 (Figure 15c), a decrease of 3.9 to 2 ppb is predicted over western San Diego, while further down wind to the east and southeast we find an increase of up to 2 ppb. In Figure 15d (July 22), the area of decrease is larger, with a smaller area of increase. The major cause of the predicted differences in O_3 levels

for the four dates are small changes in the meteorology that influence the physical and chemical processes of the different air parcels. For example for July 13, 21, and 22 the eastern part of the domain shows increased O_3 due to transport from the west, while on July 11, O_3 is higher in the north due to transport form the south.

Given this complexity of O_3 formation and the caveat that changes in emissions can lead to both formation and destruction of O_3 in different regions of the domain, for this limited period of high O_3, we find the overall contribution of DoD emission sources to the formation or titration of O_3 was found to be between +2% to -12% of the total, respectively. Further, we observe the changes to the predicted concentration of O_3 mainly occurring in and around the urban area of San Diego.

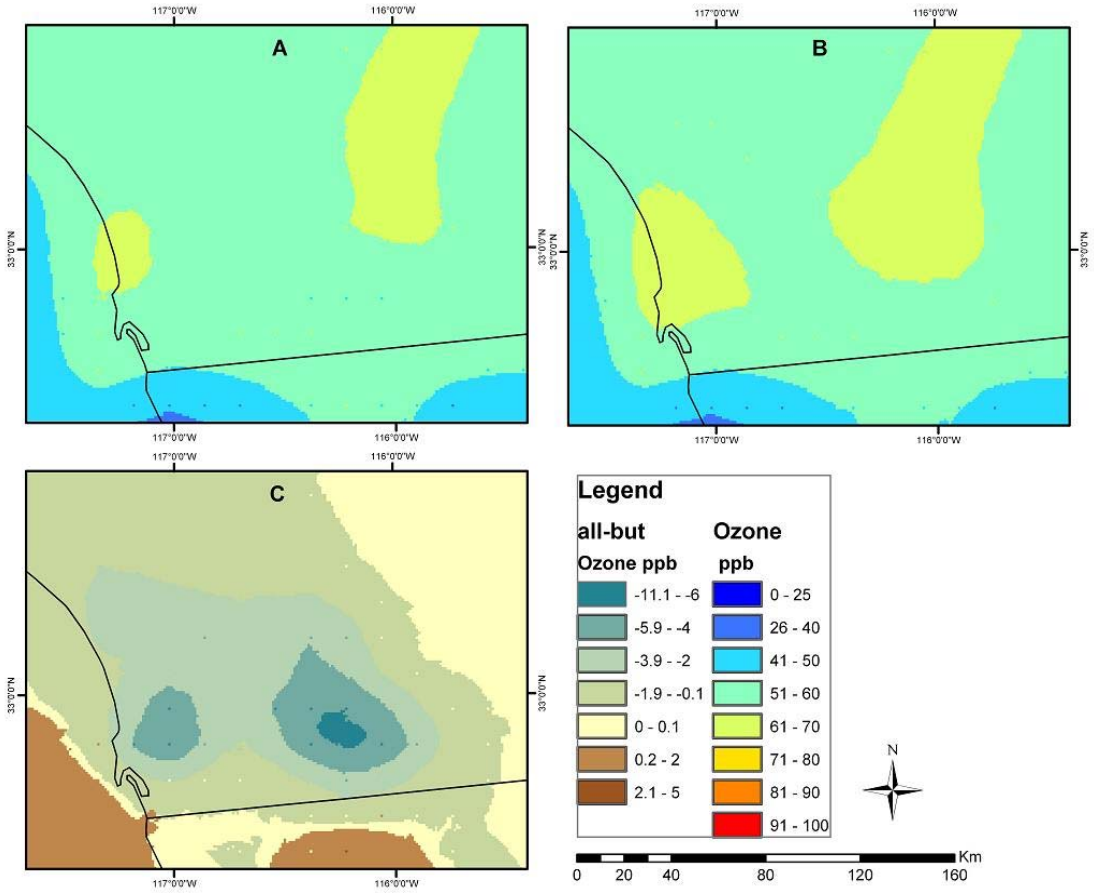

Figure 14. (a) Predicted O_3 concentration (ppb) map with all emission sources for July 19, 2003 1500 LST, (b) Same period but excluding emissions from DoD operations, and (c) Difference between (a) and (b).

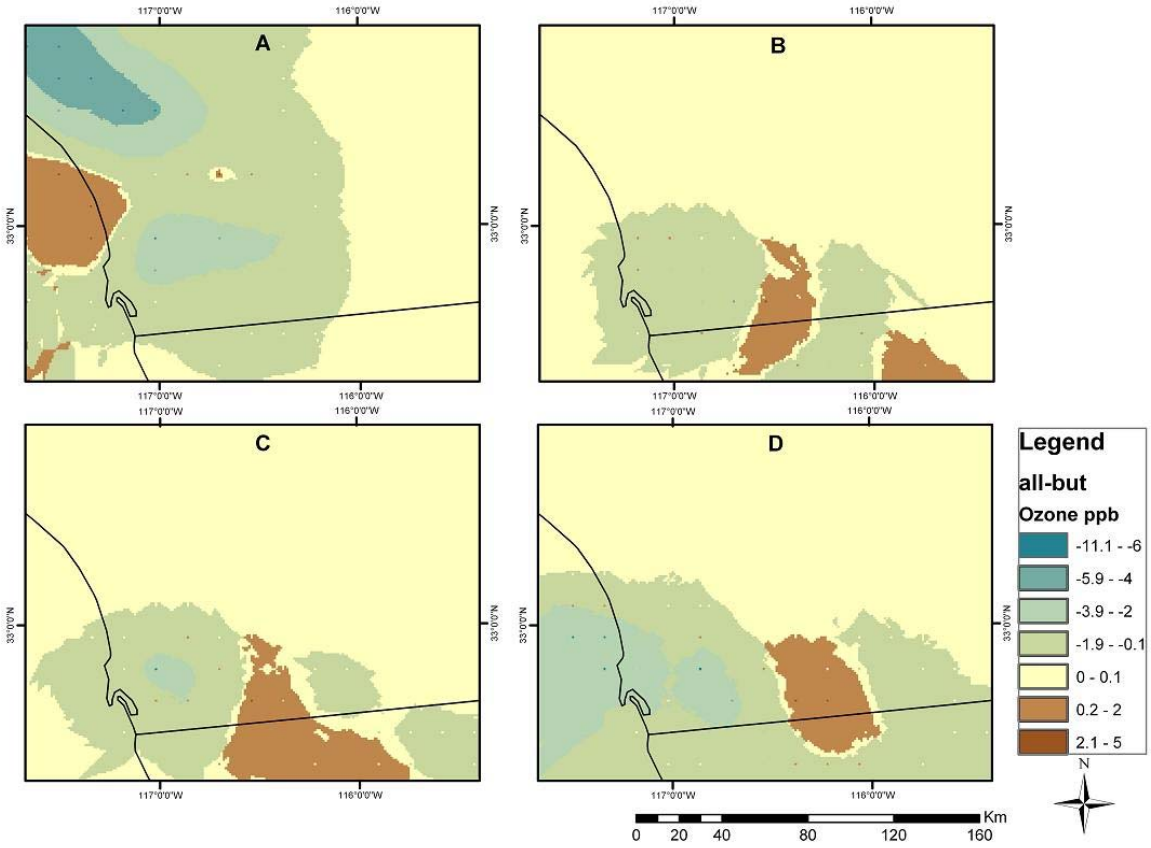

Figure 15. (a) O_3 difference map (ppb) between for simulation with all emission sources and excluding DoD operations for July 11 2003 1500 LST, (b) for July 13 2003 1500 LST, (c) for July 21 2003 1500 LST, and (d) for July 22 2003 1500 LST.

4.4 Impact of Emissions from an Individual Ship

A unique aspect of the hybrid modeling system is the ability to maintain information on emissions from each source in the domain. This enables us to determine the impact of individual sources on air quality. One of the scenarios we investigated was emissions from a single ship to assess where its plume travels and the chemical changes undergone by the emissions from this source. It should be noted that this type of scenario might be applicable to other cases of interest to DoD involving transport/dispersion and transformation in environments such as the land-sea interface and regions with complex terrain (e.g., transport of emissions from a toxic release in a harbor).

Figure 16 shows a snapshot of polluted air parcels from a ship stack at 1500 local time. The few parcels to the north (color red, 63 to 76 ppbv) are a residual part of the parcels that were transported north of the ship 7 hours earlier. Later these parcels moved to the east and reacted with other air parcels to form additional O_3. This resulted in O_3 production. When considering the dominant flow of emissions, we find that the areas around the plume have increased levels of O_3 due to the titration of O_3 with NO in the plume. While this is a test scenario, it demonstrates

the capability of the hybrid model to predict pollutant transport and transformation in the land-sea interface while maintaining information on the impact of an individual source.

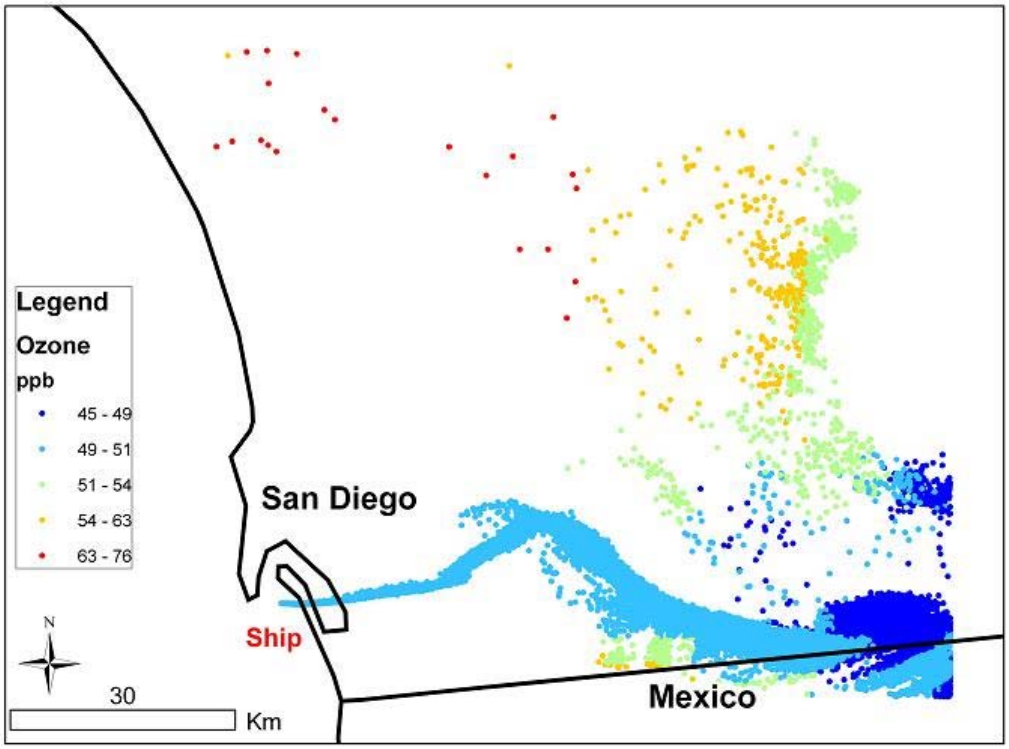

Figure 16. O_3 distribution (ppbv) due to emissions from a ship in San Diego harbor, July 7 2003 1500 LST.

5.0 Conclusions

Many of the urban areas classified as non-attainment for O_3 or PM_{10} and facing non-attainment for $PM_{2.5}$ are located along the east and west coasts of the U.S. and are home to major DoD facilities. These operations can be significant sources of the O_3 and $PM_{2.5}$ forming precursors, direct $PM_{2.5}$ and PM_{10} emissions, and emissions of toxic species. Hence there is a need to develop strategies to improve air quality while minimizing the impact on DoD operations. Much of the uncertainty in developing effective approaches to control the sources of poor air quality in these areas is uncertainty in the emissions inventories; however, in coastal areas the situation is confounded by the complex meteorology associated with the land/sea interface. While current air pollutant modeling systems can accurately predict chemical transformations under these conditions, they have difficulty predicting pollutant transport and dispersion. In order to address this issue, we developed a hybrid model that does not incorporate the chemistry module within the dispersion-advection module but rather implements the chemistry module in a post-processing mode.

The hybrid modeling system developed in this study has the following advantages:

- Incorporates the strengths of both the Lagrangian transport/diffusion model and Eulerian multi-box chemical model.
- Modular system that can readily employ alternative chemical and transport-dispersion modules.
- Capable of evaluating impact of emissions from individual sources in space and time (i.e. provides for a source/receptor relationship).
- Designed to evaluate the impact of moving sources such as ship and aircraft emissions.

As part of this program, we also performed an extensive validation of the hybrid model during a period of high O_3 over the San Diego area. This involved a series of aircraft measurements that employed a comprehensive platform for measuring emissions from individual sources and pollutant transport and transformation. In order to compare model predictions calculated on an hourly basis with the aircraft data, we developed a novel approach that involved preparing a "mosaic" of the hourly model predictions that corresponded in space and time to the aircraft observations. This methodology will enhance the applicability of future aircraft measurements for testing air quality models. In addition, the database obtained in this phase of the study can be used by others researchers to in model evaluation studies.

The model validation database enabled us to assess the impact of local and transported pollutants on air quality in the San Diego area. Findings from this component of the study included:

- Offshore sources (commercial and military vessels) can be detected through their SO_2 plume.
- The majority of SO_2 in the region is transported from sources south-southeast of San Diego, most likely from Mexico.
- Vehicular transportation is the main source of precursors leading to the formation of photochemical smog in the region.

- There is evidence of transport of O_3 and its precursors from sources in the Los Angeles area.

We also used the model to assess two scenarios of interest to DoD. These were as follows:

- The impact of DoD emissions on air quality in the San Diego area.
- The spatial and temporal impact of emissions from a single ship.

To assess the impact of DoD emissions we evaluated a number of scenarios that included eliminating all DoD emissions in the region. We found this led to both an increase and decrease in O_3 depending on location. This was due to the complex chemistry involved in O_3 formation (i.e., increasing NO emissions will decrease O_3 where the source was added while increasing O_3 further downwind). Overall, DoD emissions were found to be a small contributor to the levels of O_3 in the region.

For the investigation of the impact of emissions from a single ship, we evaluated where its plume traveled and the chemical changes undergone by the emissions from this source. We found the hybrid model was able to resolve the spatial and temporal impacts from a single source. It should be noted that this type of scenario might be applicable to other cases of interest to DoD involving transport/dispersion and transformation in environments such as the land-sea interface and regions with complex terrain (e.g., transport of a toxic release in a harbor).

As part of the transition component of this work, we have briefed a number of potential users on the results of this study. In addition to SERDP, we have presented the findings at scientific meetings and to regulatory agencies (CARB, San Diego Air Pollution Control District, and Greater Vancouver Regional District (GVRD)). CARB and GVRD have been particularly interested in using this approach to evaluate the impact of offshore emissions from ships on urban air quality.

6.0 References

Alexis, A., P. Gaffney, C. Garcia, M. Nystrom, and R. Rood (2000), *The 1999 California Almanac of Emissions and Air Quality*, California Air Resources Board, Sacramento, California.

Bauer, S. E., and B. Langmann (2002), Analysis of a Summer Smog Episode in the Berlin-Brandenburg Region with a Nested Atmosphere-Chemistry Model, *Atmos. Chem. Phys. Discuss*, *2*, 789–824.

Biswas, J., and S. T. Rao (2001), Uncertainties in Episodic Ozone Modeling Stemming from Uncertainties in the Meteorological Fields, *Journal of Applied Meteorology*, *40*, 117–136.

California Air Resources Board web site:

'http://www.arb.ca.gov/adam/cgi-bin/db2www/polltrendsb.d2w/Branch'

Corbett, J. J., and H. W. Koehler (2003), Updated Emissions from Ocean Shipping, Journal of Geophysical Research-Atmospheres, 108.

Dudhia, J. (1993), A Nonhydrostatic Version of the Penn State-Ncar Mesoscale Model: Validation Tests and Simulation of an Atlantic Cyclone and Cold Front., *Monthly Weather Review*, *121*, 1493–1513.

Dudhia, J. (2001), Mesoscale Model Nesting and Boundary Conditions, edited, National Center for Atmospheric Research, Boulder, Colorado.

Dudhia, J., and J. F. Bresch (2002), A Global Version of the PSU-NCAR Mesoscale Model, *Monthly Weather Review*, *130*, 2898-3007.

EPA (2006). www.epa.gov/oar/oaqps/greenbk/gncl8.html.

Grell, G.A., J. Dudhia and D.R. Stauffer (1994). A Description of the Fifth-Generation Penn State/NCAR Mesoscale Model (MM5). National Center for Atmospheric Research, Techn. Note TN-398, 122 pp.

Isakov, V. (1998). Evaluation of atmospheric and dispersion models in complex terrain by using tracer measurements. Ph.D. dissertation, University of Nevada, Reno, 119 pp. Available from: Desert Research Institute, 2215 Raggio Parkway, Reno, NV 89512.

Kahyaoğlu-Koračin, J. (2004), The Development and Application of Atmospheric Modeling Systems to Determine the Environmental Impact of Regional Scale and Local Emissions on Complex Mountain Terrain and Coastal-Urban Areas, 135 pp, University of Nevada, Reno.

Kahyaoğlu-Koračin, J., S. Bassett, D. Mouat, and A. W. Gertler (2006), A Scenario-Based Modeling System to Predict the Air Quality Impact from Future Growth, *Environment International*, submitted.

Koracin, D., J. Frye and V. Isakov (2000). A method of evaluating atmospheric models using tracer measurements. *J. Appl. Meteor.,* **39**, 201-221.

Koracin, D., J. Lewis, W. T. Thompson, C. E. Dorman, and J. A. Businger (2001). Transition of a stratus layer into a fog layer along the California coast: Observations and modeling. *J. Atmos. Sci,* **58**, 1714-1731.

Koracin, D., and C. Dorman (2001). Marine atmospheric boundary layer divergence and clouds along California in June 1996. *Mon. Wea. Rev*., **129**, 2040-2055.

Koracin, D., C. E. Dorman, and E. P. Dever (2004). Coastal perturbations of marine layer winds, wind stress, and wind stress curl along California and Baja California in June 1999. *J. Phys. Ocean.*, **34**, 1152-1173.

Koracin, D., Isakov, V. and D.F. Leipper (1998a). Simulations of the sea breezes on the central U.S. California coast. *Hydraulic Engineering Software*, Ed. W.R. Blain, Wessex Institute of Technology Press, Computational Mechanics Software, Ashurst, Southampton, SO40 7AA, UK, 307-316, 624pp.

Koracin, D., V. Isakov and J. Frye (1998b). A Lagrangian particle dispersion model (LAP) applied to transport and dispersion of chemical tracers in complex terrain. Presented at the Tenth Joint Conference on the Applications of Air Pollution Meteorology, Phoenix, AZ, 11-16 January 1998. Paper 5B.5, 227-230.

Koracin, D., V. Isakov, D. Podnar and J. Frye (1999). Application of a Lagrangian random particle dispersion model to the short-term impact of mobile emissions. Proceedings of the Transport and Air Pollution conference, Graz, Austria, 31 May - 2 June 1999.

Lewis, J., D. Koracin, R. Rabin, and J. Businger (2003). Sea fog off the California coast: Viewed in the context of transient weather systems. *J. Geoph. Res. (Atmos).* **108**, No. D15, 4457, 10.1029/2002JD002833.

Lewis, J., D. Koracin, and K. Redmond (2004). Sea fog research in the UK and USA: Historical essay including outlook. *Bull. Amer. Met. Soc*., **85**, 395–408.

Luria, M., R. J. Valente, N.V. Gillani, R.L. Tanner, R.E. Imhoff, and J.F. Meagher (1999). The evolution of photochemical smog in a power plant plume. *Atmos. Environ.***, 31**, 3023-3036.

Luria, M., R.L. Tanner, R.J. Valente and R.E. Imhoff (2000). The influence of natural hydrocarbons on ozone formation in an isolated power plant plume. *J. Geophys. Res.***, 105**, 9177-9188.

Luria, M., R. L. Tanner, R. J. Valente, S. T. Bairai, D. Koracin, and A. W. Gertler (2005), Local and Transported Pollution over San Diego California, Atmospheric Environment, 39, 6765-6776

Madronich, S. (1987). Photodissociation in the atmosphere: 1. Actinic flux and the effects on ground reflections and clouds. *J. Geophys. Res.,* **92,** 9740-9752.

Odman, M. T. and A.G. Russell (2002). New Techniques for Modeling Air Quality Impacts of DoD Activities. Presented at the Partners in Environmental Technology Technical Symposium and Workshop sponsored by Strategic Environmental Research And Development Program and Environmental Security Technology Certification Program, Washington, DC, December 3-5, 2002.

Pielke, R. A. (1984), *Mesoscale Meteorological Modeling*, 612 pp., Academic Press.

Rao, S. T., and G. Sistla (1993), Efficacy of Nitrogen Oxides and Hydrocarbons Emissions Controls in Ozone Attainment Strategies as Predicted by the Urban Airshed Model(Uam), *Water, Air, & Soil Pollution*, *67*, 95-116.

Seefeld, S. (1997), Laboratory Kinetic and Atmospheric Modelling Studies of the Role of Peroxyacyl Nitrates in Tropospheric Photo-Oxidant Formation, Swiss Federal Institute of Technology Zurich (ETH)

Sillman, S., D. He, M. R. Pippin, P. H. Daum, D. G. Imre, L. I. Kleinman, J. H. Lee, and J. Weinstein-Lloyd (1998), Model Correlations for Ozone, Reactive Nitrogen, and Peroxides for Nashville in Comparison with Measurements: Implications for O_3-Nox-Hydrocarbon Chemistry, *Journal of Geophysical Research-Atmospheres*, *103*, 22629-22644.

Stein, A. F., L. D., and R. R. Draxler (2000), Incorporation of Detailed Chemistry into a Three-Dimensional Lagrangian-Eulerian Hybrid Model: Application to Regional Tropospheric Ozone, *Atmospheric Environment*, *34*, 4361-4372.

Stockwell, W.R., P. Middleton, J.S. Chang, and X. Tang (1990). The second generation regional acid deposition model chemical mechanism for regional air quality modeling. *J. Geophys. Res.*, **95**, 16343-16367.

Stockwell, W.R., F. Kirchner, M. Kuhn, and S. Seefeld (1997). A new mechanism for regional atmospheric chemistry modeling. *J. Geophys. Res.*, **102**, 25847-25879.

Tesseraux, I. (2004), Risk Factors of Jet Fuel Combustion Products, Toxicology Letters, 149, 295-300.

Tory, K. J., M. E. Cope, G. D. Hess, S. Lee, K. Puri, P. C. Manins, and N. Wong (2004), The Australian Air Quality Forecasting System. Part Iii: Case Study of a Melbourne 4-Day Photochemical Smog Event., *Journal of Applied Meteorology*, *43*, 5680-5695.

Valente, R.L., R.E., Imhoff, R.L., Tanner, J.F. Meagher, P.H.Daum, R.M. Hardesty, R.V. Banta, R.J. Alvarez, R. McNider, N.V. Gillani, Ozone production during an urban air stagnation episode over Nashville, TN, *J. Geophys. Res*. **103**, 22,555-22,568, 1998.

Van Valin C.C., J.F. Boatman, M. Luria, J.D. Ray V.P. Aneja, D.R. Blake, M. Rodgers and J.T. Sigmon. Air Quality over the Appalachian Region in August 1988: A comparison between aircraft and ground based measurements**.** *J. Geophys. Res*., **99**, 1043-1057, 1994.

Weinroth, E. W. Stockwell, D. Koracin, J. Kahyaoğlu-Koračin, M. Luria, T. McCord, D. Podnar, A.W. Gertler(2005) A Hybrid Model for Local and Regional Ozone Forecasting, *Journal of Geophysical Research*, submitted

Appendix – List of Technical Publications

Peer Reviewed Publications

Luria, M., R.L. Tanner, R.J. Valente, S.T. Bairai, D. Koracin, D., and A.W. Gertler (2005). Local and Transported Pollution over San Diego California, *Atmospheric Environment*, **39**, 6765-6776.

Weinroth, E., W. Stockwell, D. Koračin, J. Kahyaoğlu-Koračin, M. Luria, T. McCord, D. Podnar, and A. Gertler (2006). A Hybrid Model for Local and Regional Ozone Forecasting, *J. Geophys Res.*, submitted.

Weinroth, E., W. Stockwell, D. Koracin, J. Kahyaoğlu-Koračin, M. Luria, T. McCord, D. Podnar, and A. Gertler (2006). Assessment the impact of military operations on air quality in San Diego, in preparation.

Proceedings

Gertler, A.W., D.R. Koracin, J.K. Koracin, J.M. Lewis, M. Luria, J.C. Sagebiel, and W.R. Stockwell (2003). Development and Validation of a Predictive Model to Assess the Impact of Coastal Operations on Urban Air Quality. Proceedings of the *26th NATO/CCMS International Technical Meeting on Air Pollution Modelling and its Application,* Istanbul, Turkey, 26-30 May 2003.

Weinroth, E., W. Stockwell, D. Koracin, J. Kahyaoğlu-Koračin, M. Luria, T. McCord, D. Podnar, A. Gertler (2005). A Predictive Model to Assess The Impact of Emissions On Urban Scale Air Quality in Coastal Regions, in *proceedings of the 3rd International Symposium on Air Quality Management at Urban, Regional and Global Scales & the 14th Regional IUAPPA Conference*, Istanbul, September 26-30, 2005.

Presentations

Gertler, A.W., D. Koracin, J. Lewis, M. Luria, J.C. Sagebiel, and W.R. Stockwell (2002). Development And Validation of a Predictive Model To Assess The Impact of Coastal Operations On Urban Scale Air Quality, Presented at the *CRC Air Toxics Modeling Workshop*, Houston, TX, February 26-27, 2002.

Gertler, A.W. (2003). Development and Validation of a Predictive Model To Assess The Impact of Coastal Operations On Urban Scale Air Quality, Presented at the *SERDP Annual In-Progress Review Meeting*, Washington, DC, 9 May 2003.

Weinroth, E., W. Stockwell, D. Koracin, J. Kahyaoğlu-Koračin, M. Luria, T. McCord, D. Podnar, A. Gertler (2005). A Predictive Model to Assess The Impact of Emissions On Urban Scale Air Quality in Coastal Regions, *presented at the 3rd International Symposium on Air Quality Management at Urban, Regional and Global Scales & the 14th Regional IUAPPA Conference*, Istanbul, September 26-30, 2005.

Gertler, A.W. (2006). Development and Validation of a Predictive Model to Assess the Impact of Coastal Zone Emissions on Urban Scale Air Quality, Chairman's Air Pollution Seminar Series, California Air Resources Board, Sacramento, CA, January 12, 2006

Posters

Gertler, A.W., D. Koracin, J. Koracin, J. Lewis, M. Luria, A. Abu-Rahmah, J.C. Sagebiel, and W.R. Stockwell (2002). Development and Validation of a Predictive Model To Assess The Impact of Coastal Operations On Urban Scale Air Quality, Presented at the *SERDP Partners in Environmental Technology Symposium,* Washington, DC, December 3 - 5, 2002.

Gertler, A.W., D.R. Koracin, J. Koracin, J.M. Lewis, M. Luria, J.C. Sagebiel, and W.R. Stockwell (2003). Development and Validation of a Predictive Model To Assess The Impact of Coastal Operations On Urban Scale Air Quality, Presented at the *26th NATO/CCMS International Meeting on Air Pollution and its Application*, Istanbul, Turkey, May 26-30, 2003.

Gertler, A.W., D.R. Koracin, J. Koracin, J.M. Lewis, M. Luria, J.C. Sagebiel, W.R. Stockwell, and R. Tanner (2003). Development and Validation of a Predictive Model To Assess The Impact of Coastal Operations On Urban Scale Air Quality, Poster presented at the *SERDP Partners in Environmental Technology Symposium,* Washington, DC, December 2 - 4, 2003.

Gertler, A.W., D.R. Koracin, J. Koracin, J.M. Lewis, M. Luria, J.C. Sagebiel, W.R. Stockwell, R. Tanner, E. Weinroth (2004). Development and Validation of a Predictive Model To Assess The Impact of Coastal Operations On Urban Scale Air Quality, Poster presented at the *SERDP Partners in Environmental Technology Symposium,* Washington, DC, November 30 – December 2, 2004

Gertler, A.W., D.R. Koracin, J. Koracin, J.M. Lewis, M. Luria, J.C. Sagebiel, W.R. Stockwell, R. Tanner, E. Weinroth (2005). Development and Validation of a Predictive Model to Assess The Impact of Coastal Operations On Urban Scale Air Quality, *presented at the SERDP Partners in Environmental Technology Symposium,* Washington, DC, November 28 – December 1, 2005.

Weinroth, E., W. Stockwell, D. Koracin, J. Kahyaoğlu-Koračin, M. Luria, T. McCord, and A. Gertler (2005). An Air Quality Chemical Postprocessor for Lagrangian Dispersion Models, *presented at the American Meteorological Society Atmospheric Sciences and Air Quality Conference*, San Francisco, CA, April 27-29, 2005.